

## Manuscript Details

**Manuscript number** BMC\_2017\_253

**Title** Bivalent O-glycoside mimetics with S/disulfide/Se substitutions and aromatic core: synthesis, molecular modeling and inhibitory activity on biomedically relevant lectins in assays of increasing physiological relevance

**Article type** Full Length Article

### Abstract

The emerging significance of recognition of cellular glycans by lectins for diverse aspects of pathophysiology is a strong incentive for considering development of bioactive and non-hydrolyzable glycoside derivatives, for example by introducing S/Se atoms and the disulfide group instead of oxygen into the glycosidic linkage. We report the synthesis of 12 bivalent thio-, disulfido- and selenoglycosides attached to benzene/naphthalene cores. They present galactose, for blocking a plant toxin, or lactose, the canonical ligand of adhesion/growth-regulatory galectins. Modeling reveals unrestrained flexibility and inter-headgroup distances too small to bridge two sites in the same lectin. Inhibitory activity was first detected by solid-phase assays using a surface-presented glycoprotein, with relative activity enhancements per sugar unit relative to free cognate sugar up to nearly 10fold. Inhibitory activity was also seen on lectin binding to surfaces of human carcinoma cells. In order to proceed to characterize this capacity in the tissue context monitoring of lectin binding in the presence of inhibitors was extended to sections of three types of murine organs as models. This procedure proved to be well-suited to determine relative activity levels of the glycoconjugates to block binding of the toxin and different human galectins to natural glycoconjugates at different sites in sections. The results on most effective inhibition by two naphthalene-based disulfides and a selenide raise the perspective for broad applicability of the histochemical assay in testing glycoclusters that target biomedically relevant lectins.

**Keywords** Agglutinin; Glycosyldisulfides; Histochemistry; Lectin; Selenoglycosides; Sugar code; Thioglycosides

**Taxonomy** Natural Product Synthesis, Biosynthesis

**Corresponding Author** Hans-J. Gabius

**Order of Authors** Herbert Kaltner, Tamás Szabó, Krisztina Fehér, Sabine André, Sára Balla, Joachim C. Manning, László Szilágyi, Hans-J. Gabius

**Suggested reviewers** Jayaraman Narayanaswamy, Patrick Rollin, Goreti Ribeiro Morais, Stefan Oscarson, Rocco Ungaro

## Submission Files Included in this PDF

### File Name [File Type]

Cover letterdocx.docx [Cover Letter]

Letter-Waldmann-Revision.docx [Response to Reviewers]

graphical abstract.jpg [Graphical Abstract]

manuscriptcomplete-nnew.docx [Manuscript File]

Chart1\_corr.docx [Figure]

Chart2A\_corr.docx [Figure]

Chart2B\_corr.docx [Figure]

Fig1\_corr.docx [Figure]

Fig\_2.tif [Figure]

Fig\_3.tif [Figure]

Fig\_4.tif [Figure]

Fig\_5.tif [Figure]

Fig\_6.tif [Figure]

checklistcompounds.xls [Checklist]

Highlights.docx [Highlights]

Supporting\_Info\_NMRSpectra.docx [Supporting File]

To view all the submission files, including those not included in the PDF, click on the manuscript title on your EVISE Homepage, then click 'Download zip file'.

**Bivalent *O*-glycoside mimetics with *S/disulfide/Se* substitutions and aromatic core:  
synthesis, molecular modeling and inhibitory activity on biomedically relevant lectins in  
assays of increasing physiological relevance**

Herbert Kaltner,<sup>a,\*</sup> Tamás Szabó,<sup>b,c,\*</sup> Krisztina Fehér,<sup>d</sup> Sabine André,<sup>a</sup> Sára Balla,<sup>b</sup> Joachim C. Manning,<sup>a</sup> László Szilágyi<sup>b,#</sup> and Hans-Joachim Gabius<sup>a,#</sup>

<sup>a</sup>Institute of Physiological Chemistry, Faculty of Veterinary Medicine, Ludwig-Maximilians-University Munich, Veterinärstr. 13, 80539 München, Germany

<sup>b</sup>Department of Chemistry, University of Debrecen, PO Box 20, 4010 Debrecen, Hungary

<sup>c</sup>Richter Gedeon Rt., Gyömrői út 19-21, 1103 Budapest, Hungary

<sup>d</sup>NMR and Structural Analysis Unit, Department of Organic and Macromolecular Chemistry, Ghent University, Krijgslaan 281, 9000 Ghent, Belgium

\*contributed equally

Running title

S/Se glycomimetics as lectin inhibitors

# Corresponding authors

Tel.: +36 52 512900x22589; fax: +36 52 512747x23744. *E-mail address:*

[lszilagy@unideb.hu](mailto:lszilagy@unideb.hu)

Tel.: +49 89 2180 2290; fax: +49 89 2180 992290. *E-mail address:* [gabius@tiph.vetmed.uni-muenchen.de](mailto:gabius@tiph.vetmed.uni-muenchen.de), [gabius@lectins.de](mailto:gabius@lectins.de)

**Abstract** – The emerging significance of recognition of cellular glycans by lectins for diverse aspects of pathophysiology is a strong incentive for considering development of bioactive and non-hydrolyzable glycoside derivatives, for example by introducing *S/Se* atoms and the disulfide group instead of oxygen into the glycosidic linkage. We report the synthesis of 12 bivalent thio-, disulfido- and selenoglycosides attached to benzene/naphthalene cores. They present galactose, for blocking a plant toxin, or lactose, the canonical ligand of adhesion/growth-regulatory galectins. Modeling reveals unrestrained flexibility and inter-headgroup distances too small to bridge two sites in the same lectin. Inhibitory activity was first detected by solid-phase assays using a surface-presented glycoprotein, with relative activity enhancements per sugar unit relative to free cognate sugar up to nearly 10fold. Inhibitory activity was also seen on lectin binding to surfaces of human carcinoma cells. In order to proceed to characterize this capacity in the tissue context monitoring of lectin binding in the presence of inhibitors was extended to sections of three types of murine organs as models. This procedure proved to be well-suited to determine relative activity levels of the glycoconjugates to block binding of the toxin and different human galectins to natural glycoconjugates at different sites in sections. The results on most effective inhibition by two naphthalene-based disulfides and a selenide raise the perspective for broad applicability of the histochemical assay in testing glycoclusters that target biomedically relevant lectins.

**Key words:** Agglutinin; Glycosyldisulfides; Histochemistry; Lectin; Selenoglycosides; Sugar code; Thioglycosides

## 1. Introduction

A prominent hallmark of cell surfaces is the presentation of a wide array of glycans by cellular glycoconjugates. They are produced by intimately controlled and regulated glycosylation, often likened to a cell's fingerprint that undergoes profound developmental and disease-associated alterations.<sup>1-6</sup> Our view on the glycans' (patho)physiological significance has matured from an initial interpretation as purely phenomenological markers to the current delineation of their nature as meaningful biochemical signals that harbor information encoded in sequence and shape, the basis of the concept of the sugar code.<sup>7-10</sup> One route of translating this information into bioeffects is via functional pairing with sugar receptors (lectins), what explains the increasing attention to study protein-glycan recognition.<sup>11-13</sup>

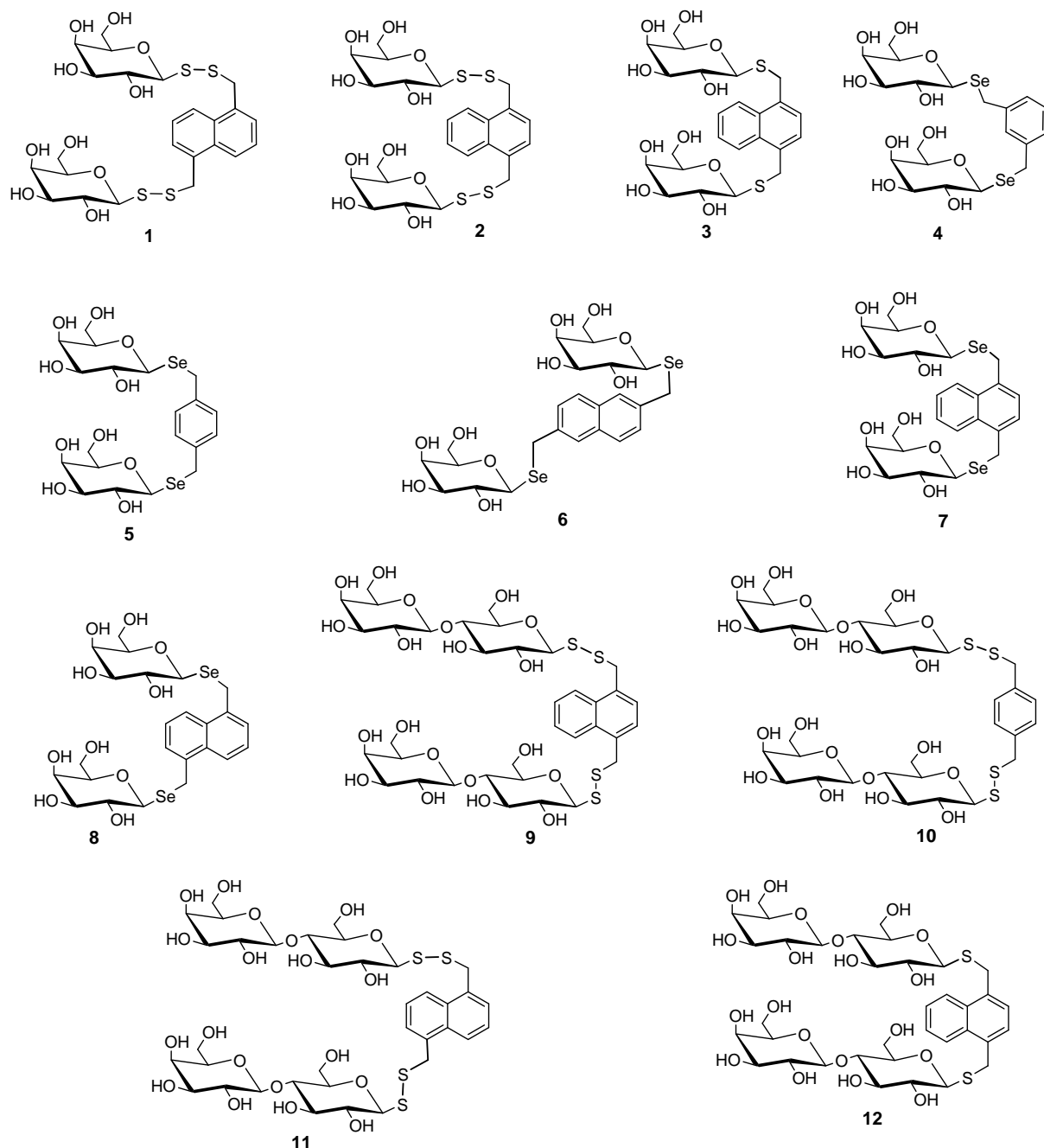
The available body of evidence underscores that the reactivity of glycans for lectins *in situ* critically depends on the presentation of the cognate epitope in a topologically suited manner, for example by branched *N*- or *O*-glycans or by microdomains in membranes. This interplay of complementary features on several levels sets limits for the expectation that binding partners in artificial laboratory assays will necessarily have the same characteristics as the operative counterreceptors on/in cells. In fact, the emerging insights into the remarkable selectivity of lectins for few distinct targets from the broad panel of cellular glycoconjugates give a strong incentive to work with synthetic cluster glycosides to measure the impact of topological properties.<sup>14-16</sup> Preferably, these compounds should have a glycosidic linkage that is resistant to hydrolysis by glycosidases, hereby enabling to consider a perspective for application as stable pharmaceutical inhibitor against toxins or harmful activities of tissue lectins. However, such a substitution, for example from oxygen in inter-residual bonds to thio- or selenoglycosidic linkages, entails alterations in bond angles ( $C-C-O$ :  $115^\circ$ ;  $C-C-S/Se$ :  $95^\circ$ ) and length ( $C-O$ :  $1.4 \text{ \AA}$ ;  $C-S$ :  $1.8 \text{ \AA}$ ;  $C-Se$ :  $1.9 \text{ \AA}$ ). These changes raise the question on the capacity of the resulting products as competitive inhibitor of lectin binding to counterreceptors. This parameter is routinely tested by engaging glycoconjugates as assay platform, for example a glycoprotein. To meet the challenge of including topological features, established cell lines, commonly used for functional assays, offer an attractive system of increased relevance, and, indeed, work on the role of adhesins in pathogen-host recognition has recently emphasized "the critical importance of utilizing physiologically relevant cells".<sup>17</sup> In order to monitor reduction of lectin binding to cells and the extracellular matrix in a single experimental setting in the tissue context, we here proceed to work with tissue sections.

Thio- and dithioglycosides have gained special interest due to the thiol-disulfide conversion in dynamic combinatorial libraries of thioglycosides, broadened to the level of glycopeptides and -proteins.<sup>18-21</sup> The facile preparation of symmetric glycosyldisulfides, in parallel, contributed to start exploring their bioactivity profiles.<sup>22-25</sup> Remarkably, glycosyldisulfides, especially dithiodigalactoside, have already been identified as inhibitors for biomedically relevant plant agglutinins and, albeit less potently, human lectins,<sup>26, 27</sup> and, more recently, seleno- and diselenodigalactosides have been found to share this property.<sup>28</sup> In this report, first the synthesis of a panel of 12 bivalent benzene- or naphthalene-based thio-, disulfido- and selenoglycoside derivatives (Chart 1) is described. Running molecular-modeling protocols answers the question on the accessible conformational space, solid-phase lectin assays on potential for bioactivity by reduction of extent of binding to a glycoprotein by a plant toxin, i.e. *Viscum album* agglutinin,<sup>29</sup> or by human adhesion/growth-regulatory galectins.<sup>30</sup> Finally, the cell biological and histochemical experiments, using free sugar as control in parallel, determine this capacity, when the lectins are bound by cognate glycoconjugates on surfaces of tumor cells in culture as well as of cells and matrix in sections of fixed organ specimens.

## 2. Results and discussion

### 2.1. Chemistry

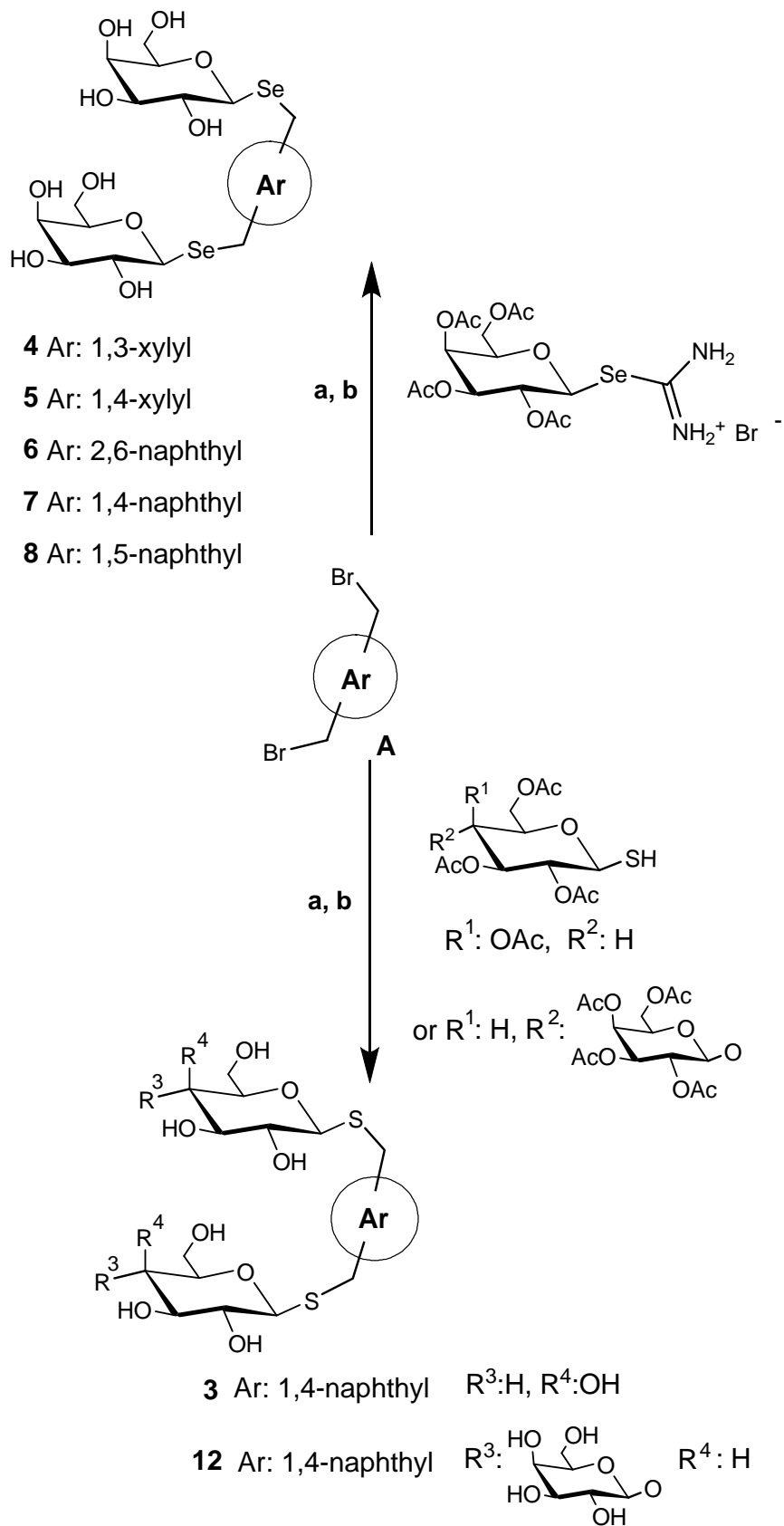
The panel of bivalent compounds is divided into the group of  $\beta$ -galactoside-presenting derivatives **1-8** for testing with the plant toxin and the lactose-containing compounds **9-12** (Chart 1). Naphthalene-based disulfides **1** and **2** and the thioglycoside **3** as well as the benzene- (**4, 5**) and naphthalene-based selenides (**6-8**) constitute the first group. Disulfides of aromatic cores (**9-11**) and a naphthalene-based thioglycoside derivative (**12**) establish the second group for testing binding to human galectins.



**Chart 1** Structures of thio-, disulfido- and selenoglycoside derivatives **1-12**

The synthetic routes are summarized in Chart 2. As illustrated, the selenoglycosides **4-8** were prepared via reactions of bis(bromomethyl)benzenes or -naphthalenes (**A**) with 2,3,4,6-tetra-*O*-acetyl- $\beta$ -D-galactopyranosyl *iso*selenuronium bromide<sup>28</sup> according to a published procedure<sup>31</sup> followed by deacetylation. Similar reactions with 1-thio-2,3,4,6-tetra-*O*-acetyl- $\beta$ -D-galactopyranose<sup>32, 33</sup> and 1-thio-2,3,6-tri-*O*-acetyl-4-(2,3,4,6-tetra-*O*-acetyl- $\beta$ -D-galactopyranosyl)- $\beta$ -D-glucopyranose<sup>34</sup> resulted in the formation of compounds **3** and **12** after deacetylation. Aromatic bis(methanethiosulfonates) (**B**) provided the fully acetylated compounds **1, 2, 9, 10** and **11**, which were deprotected by treatment with equivalent LiOH in

methanol. It is worth noting that the core's extension from benzene to naphthalene can readily facilitate fluorescence measurements, and previous analysis of a respective lactose derivative with such an appendix has excluded a primarily non-specific (hydrophobic) binding to galectins.<sup>35</sup> In order to gain insights into the accessible conformational space of the sugar headgroups attached to these aromatic cores, we performed molecular modeling.



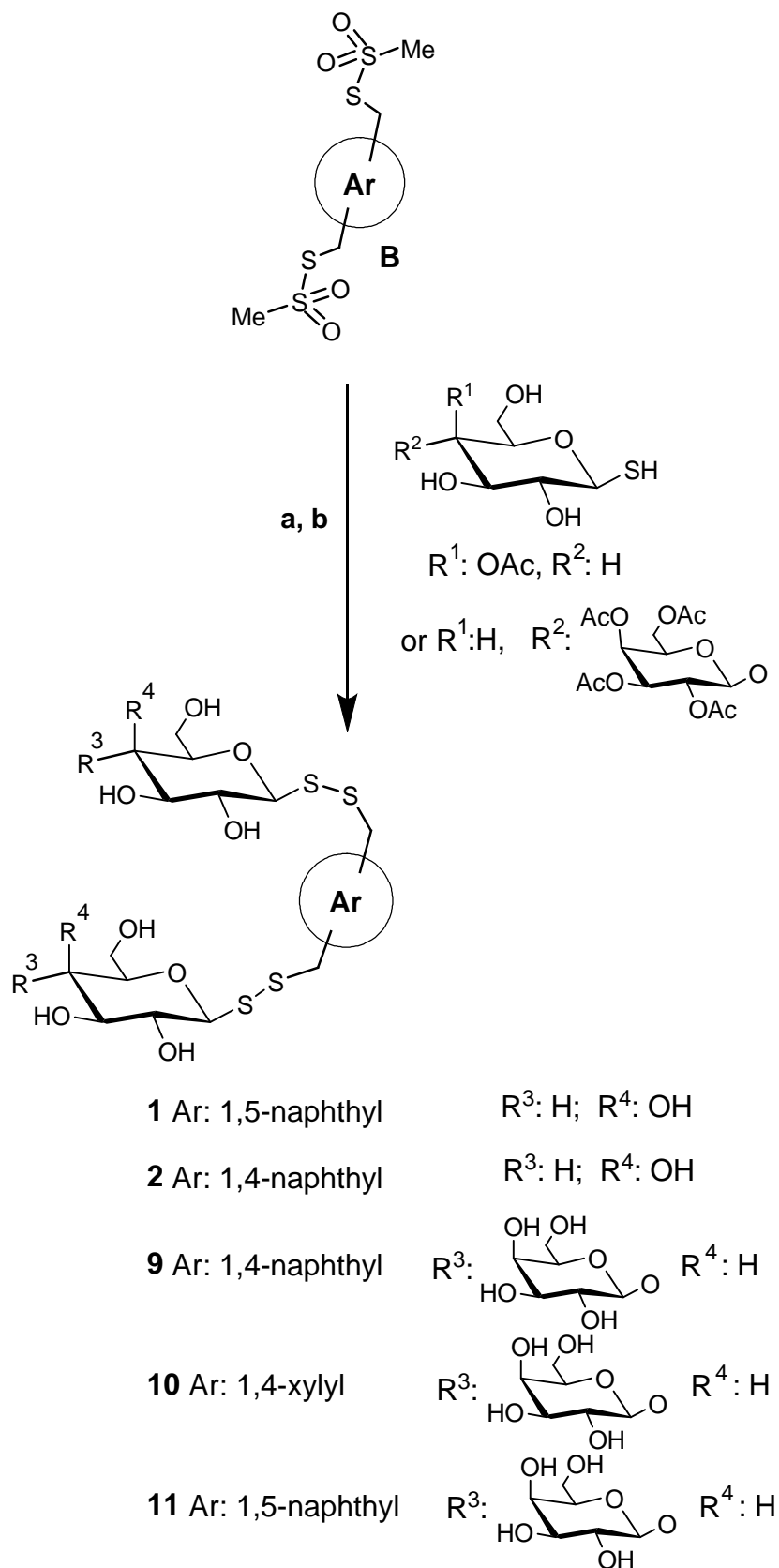


**Chart 2** Syntheses of thio- and seleno derivatives 1-12

## 2.2. Molecular modeling

Conformational parameters were computationally calculated exemplarily for the benzene-based selenides **4** and **5** and the naphthalene-based disulfides **9** and **11** to infer any impact of positional effects (*meta* or *para*) on headgroup presentation. The models (built in Discovery Studio Visualizer 4.5 (Biovia)) for each compound were subjected to molecular dynamics (MD) calculations using General Amber Force Field (GAFF) in the AMBER14 simulation protocol at 298 K for 100 ns, with addition of an octahedral shell of explicit water molecules around the glycoside derivatives implemented in each case. A set of 10,000 structures was retained, all of which were analyzed.

In order to comparatively characterize the individual arrangements of the two pairs, three parameters were selected for documentation: i) the inter-headgroup separation of sugar units as defined by the distance between anomeric carbon centers, ii) the orientation of the lactose units by a pseudo torsion angle defined between the C4 atoms of galactose and the C1 atoms of glucose moieties, respectively, and iii) the orientation of galactose units by a pseudo torsion angle defined between the bond vectors of O4-C4 in galactose residues. The distance between the two sugar units in each pair was within the range of 4 Å to 11 Å (Fig. 1a, c, e, g). Obviously, the substitution pattern can slightly shift the distance profile, the *meta*-constellation yielding smaller distances than a *para*-substitution. This information can be set into relation to the distances between carbohydrate-binding sites in lectins. Since the two contact regions characterized by the central Trp residues are at least 15 Å apart,<sup>36</sup> a bridging of contact sites by a bivalent compound is hardly possible. Such a scenario has been reported for wheat germ agglutinin (WGA), where pairs of the total of eight adjacent binding sites were loaded by four fitting bivalent compounds.<sup>37</sup> Interestingly, the same aim, that is high avidity to the lectin, had also been attained by cross-linking several WGA molecules.<sup>38</sup> Such a mechanism could be affected in efficiency by restrictions in flexibility.

The scatter plots of pseudo torsion angles, shown in Fig. 1b, d for galactose-presenting compounds **4** and **5** and in Fig. 1f, h for lactose-presenting compounds **9** and **11**, revealed accessibility to nearly the entire conformational space, with some preferences indicated by clustering. The results are in line with modeling of selenoglycosides using a force field version adapted for selenoglycosides that revealed similarities to the flexibility of thioglycosides.<sup>39</sup> The headgroups are thus presented by both types of aromatic core in a

flexible and dynamic manner, making lectin binding likely. This parameter is first assessed systematically by a solid-phase assay.

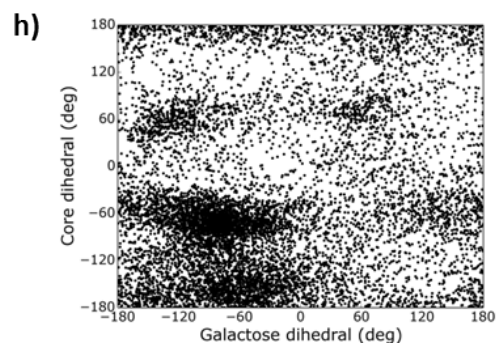
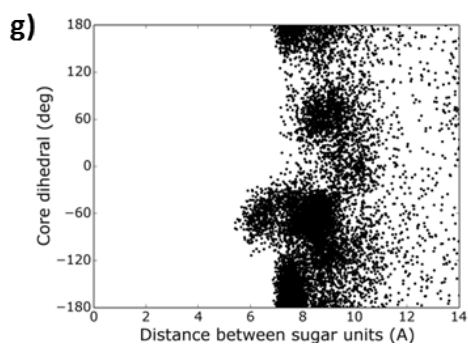
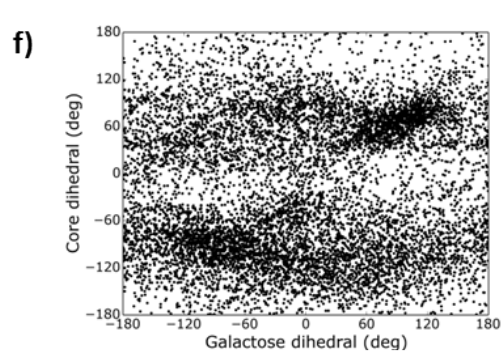
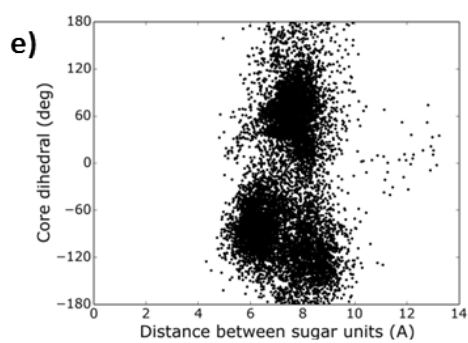
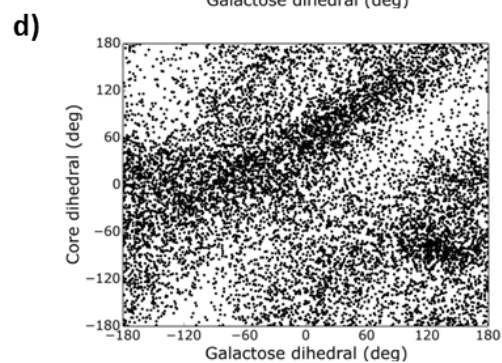
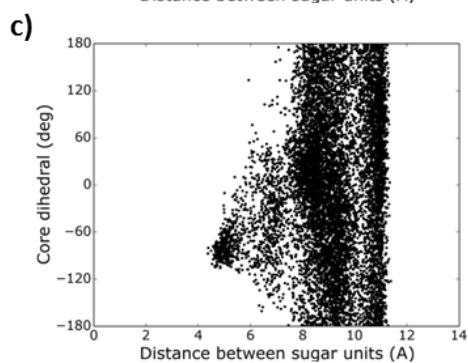
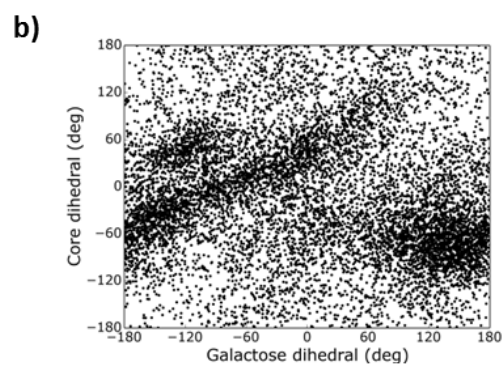
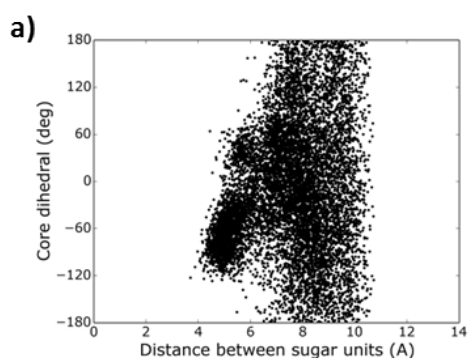
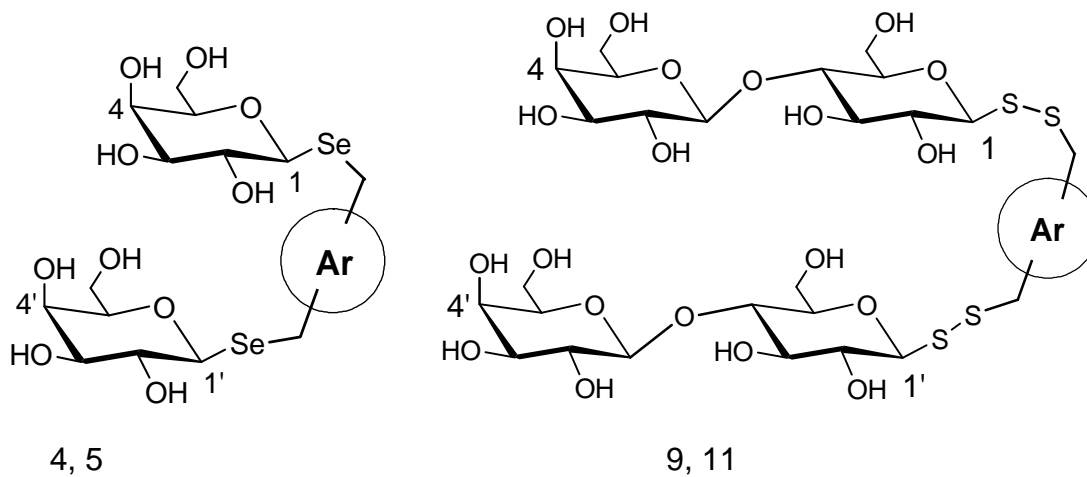


**Figure 1.** Geometric parameters to define distances between and relative orientations of sugar units obtained by molecular dynamics simulations for **4** (a & b), **5** (c & d), **9** (e & f) and **11** (g & h). The plots depict changes of the separation between sugar units as defined by C1-C1' distance (in Å) of galactose units in **4** & **5** (a & c) and that of glucose residues of the lactose units in **9** & **11** (e & g) as a function of the pseudo torsion angles (in deg) as defined by GalC4-GalC1-GalC1'-GalC4' for **4** & **5** and by GalC4-GlcC1-GlcC1'-GalC4' for **9** & **11**, respectively, denoted as the “core dihedral”; as well as variations of the pseudo torsion angles defined by the GalC4-GalO4-GalC4'-GalO4' denoted as the “galactose dihedral” as a function of the core dihedrals for **4** & **5** (b & d) and for **9** & **11** (f & h).

### 2.3. Inhibition assays

A glycoprotein with up to nine binding sites for the tested lectins, i.e. asialofetuin (ASF), is adsorbed to the surface of microtiter plate wells. As consequence, a matrix is established for binding of labeled lectins by *N*-acetyllactosamine termini of the glycoprotein's branched *N*-glycans. The association of lectin to the glycoprotein is nearly completely inhibitable by cognate sugar, ascertaining its nature by glycan recognition, as demonstrated before in precipitation assays that yielded the expected 1:9 stoichiometry of ASF/VAA complexes at lectin saturation.<sup>40</sup> Bound lectin is quantitated spectrophotometrically. Free galactose served as reference to determine the relative increase in inhibitory capacity by bivalent presentation. To avoid any turbidity of solutions compounds were in those cases first dissolved in DMSO, this clear solution then slowly added to buffer. However, aggregate formation cannot be excluded. Controls were then also run with the same final concentration of the aprotic solvent. Compounds **1** to **8** invariably proved to enhance the inhibitory capacity of free galactose by a factor from 2.5 up to nearly 10fold. The disulfide **2** and the selenide **6** reached highest levels in this respect, encouraging to test inhibition of lectin binding to cultured cells. When VAA formed contact to glycans on cell surfaces, the same tendency was observed, as shown in Fig. 2a,b for compound **2** relative to galactose presented by two other scaffolds. This result confirms and extends previous experience with different structural modes for attaining bivalency.<sup>41-45</sup> It qualifies these two compounds for the ensuing histochemical assay.

Activity was similarly examined in the solid-phase and cell assays for endogenous lectins with compounds **9** - **12**. Among the human galectins, proto-type (homodimeric) galectin-1, chimera-type galectin-3 and tandem-repeat-type galectin-8, representing the three modes of structural galectin design, are the most prominently studied members of this family.<sup>46-48</sup> Disease progression in osteoarthritis is a clinical example of harmful effects of these three

lectins.<sup>49-51</sup> Disulfide **9** proved most active as inhibitor of glycoprotein binding in all three cases, whereas for example the thioglycoside **12** conveyed comparatively less increase of inhibitory capacity to lactose by conjugation to the scaffold. When testing the effect of presence of the cognate sugar on cell binding, the same tendency was seen. Figure 2c illustrates the superior inhibitory potency of compound **9** vs free lactose on galectin-3, Fig. 2d,e on homodimeric wild-type galectin-1 and a covalently linked variant of this lectin and Fig. 2f on galectin-8. These observations explain why compound **9**, together with a control (here compound **12**), was taken to the histochemical evaluation of inhibition. In this assay, the labeled lectin will bind to reactive sites in the tissue section (control), and an inhibitor will decrease signal intensity in the specimen according to its capacity for competition with the underlying molecular interaction of the lectin with the different sites of positivity in the organ, all examined at the same time in the same section.

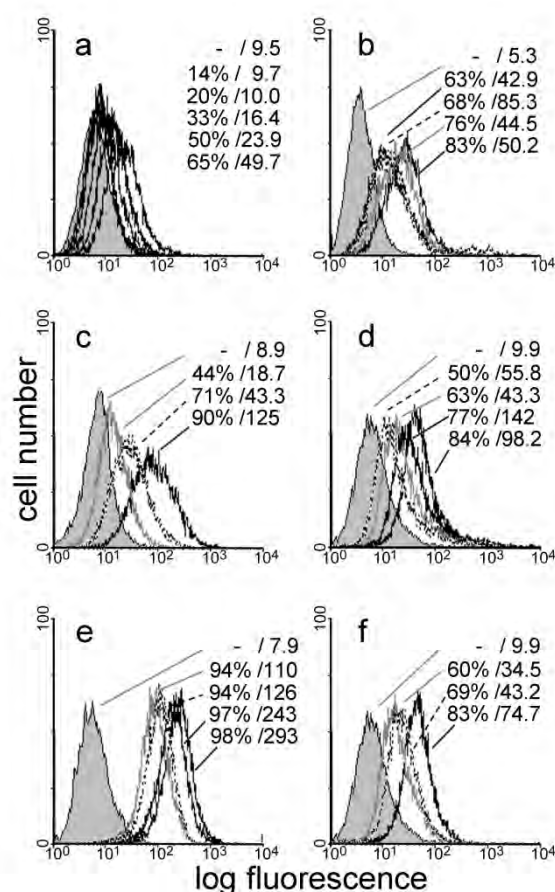


**Figure 2.** Flow cytometric analysis of extent of inhibition of lectin binding to cell surface glycans (tested on the human colon adenocarcinoma line SW480 (a-c) and the pancreatic carcinoma line Capan-1 reconstituted for expression of the human tumor suppressor p16<sup>INK4a</sup> (d-f)) by cognate sugar, free or as part of bivalent glycoconjugates. Numbers in each panel give percentage of positive cells/mean fluorescence intensity, the grey curve represents the 0%-level (background control) in the absence of labeled lectin (set of numbers given on top of list in the right part of each illustration). VAA-dependent staining when increasing lectin concentration from 0.1  $\mu\text{g}/\text{mL}$  to 0.2  $\mu\text{g}/\text{mL}$ ,

0.5 µg/mL, 1 µg/mL and 2 µg/mL (a) and with lectin (2 µg/mL fluorescent lectin) in the presence of 0.5 mM galactose presented by compound **2**, of 2 mM by compound **8** and of 0.5 mM by compound **3** as well as in the absence of cognate sugar (100%-level) (curves from left to right, numbers in list from top to bottom) (b). Galectin-3-dependent staining (10 µg/mL biotinylated lectin) in the presence of 0.1 mM lactose presented by compound **9** and as free sugar as well as in the absence of sugar (c). Galectin-1-dependent staining (20 µg/mL fluorescent lectin) in the presence of 10 mM free lactose and of 1 mM lactose presented by compounds **9** and **11**, respectively, as well as in the absence of sugar (d). Staining by the engineered galectin-1 variant with covalent connection of the two lectin domains (2 µg/mL fluorescent lectin) in the presence of 2 mM lactose presented by compound **9**, 10 mM free lactose and 2 mM lactose presented by compound **11** as well as in the absence of sugar (e). Galectin-8-dependent staining (2 µg/mL fluorescent lectin) in the presence of 2 mM lactose presented by compound **9** and 10 mM free lactose as well as in the absence of sugar (f).

In the first stage of running this assay, staining was proven to be dependent on the presence of the labeled lectin and to be inhibitable by blocking lectin binding with cognate sugar.

Galactose/lactose can completely block positivity so that lectin-independent mechanisms for signal generation could be excluded. The optimal concentration of labeled lectin, at which the signal-to-background ratio was best, was determined by systematically processing serial sections using stepwise increases from a broad concentration range of each lectin, i.e. 0.2-4 µg/mL for VAA, 0.5-6 µg/mL for galectin-3, 0.125-2 µg/mL for galectin-1 and 0.25-2 µg/mL for galectin-8. These experiments establish the 100%-value and ensure inhibitability of binding by cognate sugar.

To illustrate the principle of this assay, results from systematic titrations with inhibitor in the case of labeled VAA and sections of fixed adult murine kidney are presented in Fig. 3.

Stepwise increases of the concentration of free cognate sugar (galactose) led to corresponding decreases of positivity, from 100% to no binding, and a value of about 5 mM free galactose as inhibitory concentration to reduce signal intensity to 50% (IC<sub>50</sub>-value) (Fig. 3a-d). In comparison to the total experimental read-out in the two assays given above, microscopical evaluation of each section enables monitoring of various tissue constituents, that is the different cell types and extracellular matrix. Figure 3d provides the 0%-value for internal calibration.

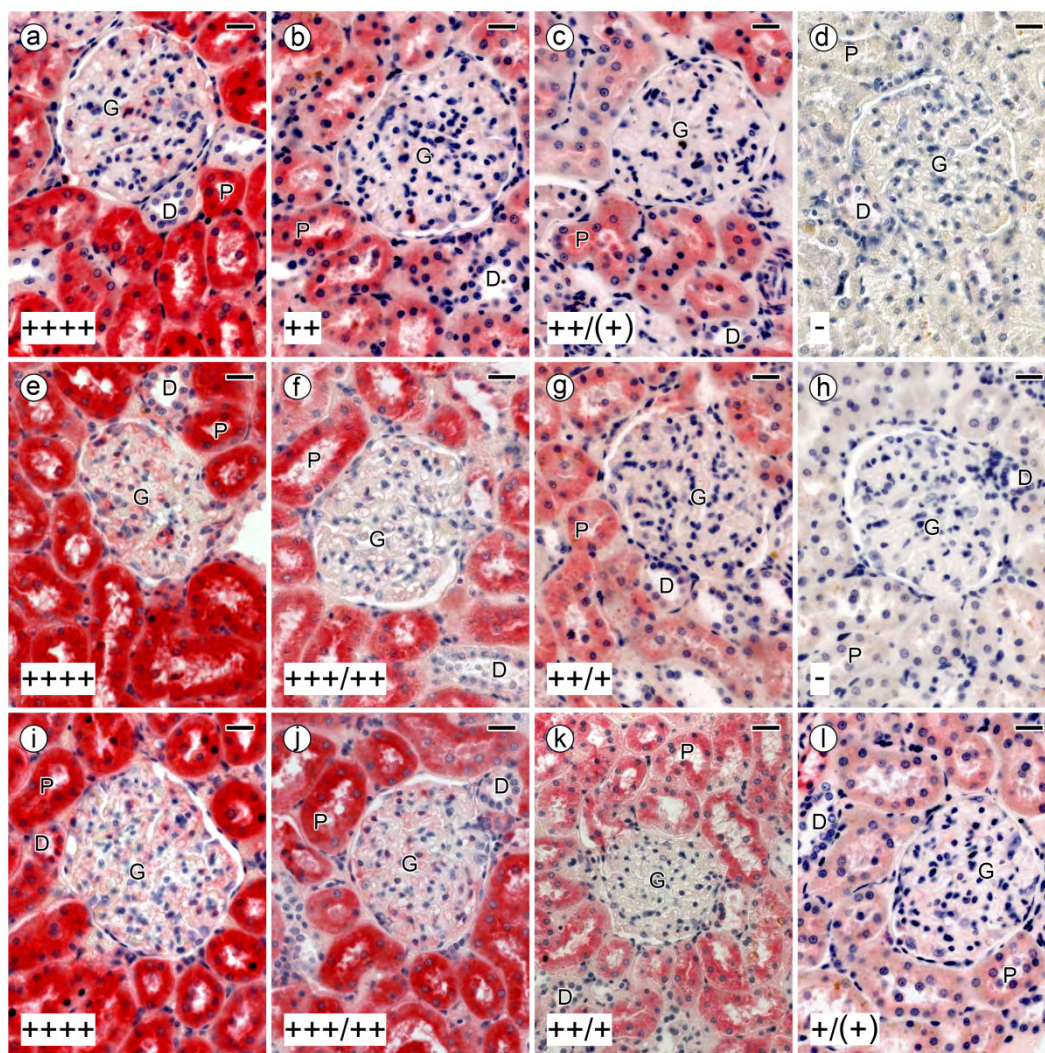


**Figure 3.** Stepwise reduction of VAA-dependent staining in sections of fixed adult murine kidney by presence of increasing concentrations of cognate sugar (galactose). The lectin (at 1  $\mu\text{g}/\text{mL}$ ) bound strongly to epithelial lining and brush border of proximal tubules (P), whereas glomeruli (G) and distal tubules (D) remained mostly unstained. In titrations, the 100%-level of signal intensity was still obtained in the presence of 2 mM free galactose (a) and 0.1 mM of scaffold-presented galactose (by compound **2**: e; by compound **6**: i). Increases of sugar concentration (5 mM (b), 10 mM (c) and 50 mM (d) of free galactose; 0.5 mM (f, j), 1 mM (g, k) and 5 mM (h, l) galactose in disulfide **2** (e-h) and selenide **6** (i-l)) led to increasing degrees of inhibition of lectin binding. The corresponding category of signal intensity after semiquantitative grading is given in the bottom left part of each microphotograph, following intensity assessment according to the following system: -, no staining; (+), very weak but significant staining; +, weak staining; ++, medium-level staining; +++, strong staining; +++++, very strong staining. Scale bars: 20  $\mu\text{m}$ .

Tested as inhibitor on toxin binding, compounds **2** and **6** were rather similarly active with  $\text{IC}_{50}$ -values between 0.5 mM and 1 mM galactose (Fig. 3e-l), relative to the 5 mM value for free galactose. Broadening the experimental basis to two further organs, sections of murine epididymis (Fig. 4a-d), thoroughly studied with VAA previously<sup>52</sup>, and jejunum (Fig. 4e-h) were subjected to respective processing. As illustrated in Fig. 4 by presenting  $\text{IC}_{50}$ -

constellations, relative potency grading was similar. It is important to note that the microphotographs should be closely examined in all regions: signals in the striated border of epithelial cells in jejunum were significantly more susceptible to intensity decrease by compound presence than to presence of free galactose (Fig. 4e-h). The detection of such a regional disparity is a clear advantage of this assay. As the plant lectin does, tissue (endogenous) lectins also yield staining patterns, which depend on the nature of the lectin (for histological details, please see legend to figures).

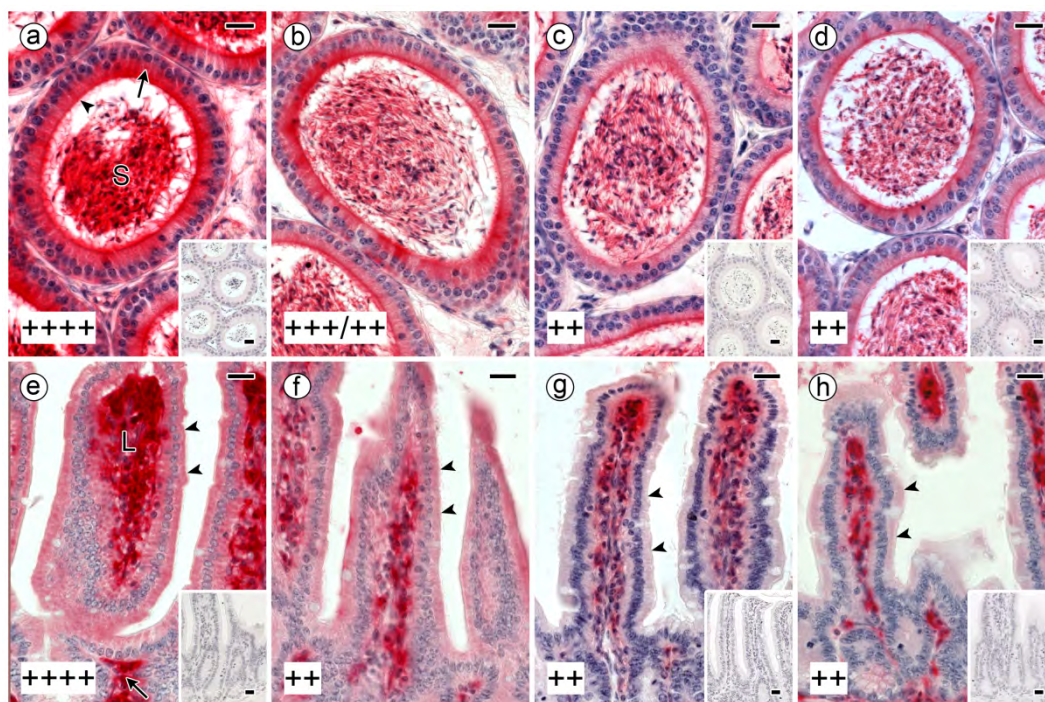


**Figure 4.** Stepwise reduction of VAA-dependent staining in sections of the corpus region of fixed murine epididymis (a-d) and of jejunum (e-h) by presence of increasing concentrations of cognate sugar (galactose). The lectin (at 1  $\mu\text{g}/\text{mL}$ ) bound strongly to the epithelial lining of ductus epididymidis, here especially in the supranuclear area of principal cells (arrow), also to stereocilia on the luminal surface of principal cells (arrowhead) and luminal spermatozoa (S), shown in a. In jejunum, shown in e, lamina propria mucosae of villi intestinales (L) and glandulae intestinales (arrow) were main sites of strong signal intensity. No reduction of signal intensity was seen in the presence of up to 1 mM free galactose (a, e). For the two organs, presence of 5 mM/10 mM free galactose (b/f), of 0.5 mM/1 mM galactose presented by compound **2** (c/g) or 0.25 mM/1 mM galactose presented by compound **6** (d/h) inhibited lectin binding by about 50%. Staining of the striated border and cytoplasm of the epithelial lining (arrowheads) appears less affected by lactose (f) than by the lactoside derivatives (g, h). Complete inhibition was obtained at 50 mM free galactose (insets to a, e) and at 10 mM of scaffold-presented galactose (insets to c, g and to d, h). Scale bars: 20  $\mu\text{m}$ .

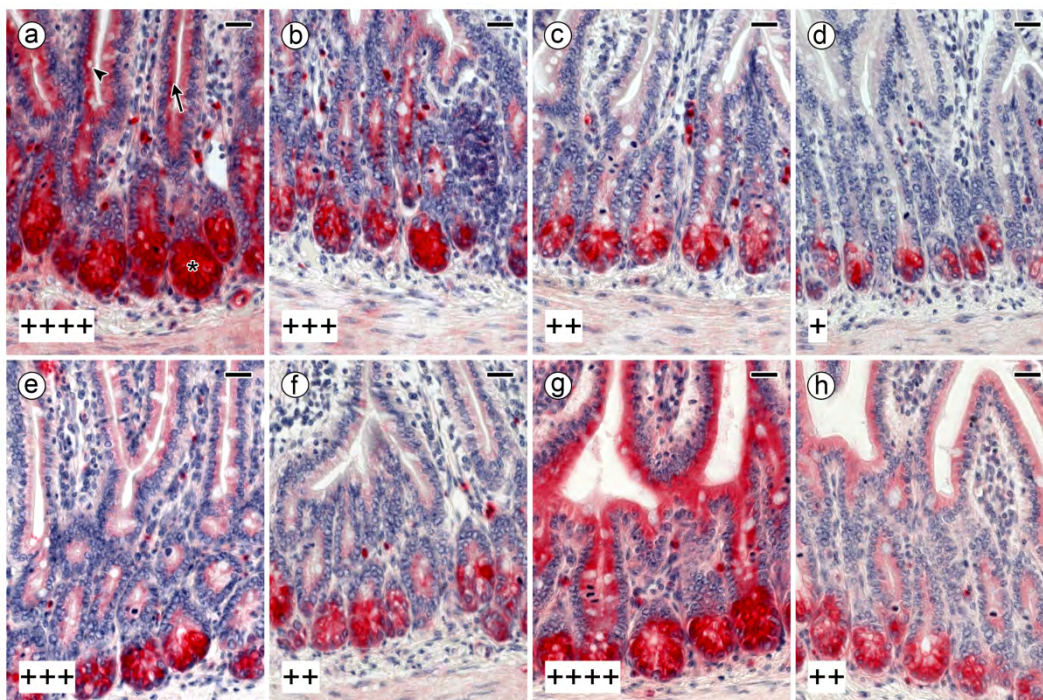


**Figure 5.** Stepwise reduction of galectin-3-dependent staining in sections of fixed murine jejunum by presence of increasing concentrations of cognate sugar (lactose). The lectin (at 4  $\mu\text{g}/\text{mL}$ ) bound strongly to epithelial cells in glandulae intestinales (asterisk) and also to the apical part of epithelial cells in villi intestinales (arrow). Goblet cells, in contrast, were negative (arrowhead). Staining intensity remained at the 100%-level in the presence of up to 5  $\mu\text{M}$  lactose presented by compound **9** (a) and decreased when increasing the sugar concentration to 10  $\mu\text{M}$  (b), 25  $\mu\text{M}$  (c) and 50  $\mu\text{M}$  (d). Testing the  $\text{IC}_{50}$  of lactose for this compound (at 25  $\mu\text{M}$  of lactose) presented by compound **12** (e) and for free lactose (g) revealed less (e) or no (g) effect. The concentration for reaching 50%-level was 50  $\mu\text{M}$  for the thioglycoside **12** (f) and 1 mM for free lactose (h). Scale bars: 20  $\mu\text{m}$ .

In the case of galectin-3, the  $\text{IC}_{50}$ -value of compound **9** for reducing signal intensity in sections of fixed murine jejunum was about 25  $\mu\text{M}$  (Fig. 5a-d). Respective values were 50  $\mu\text{M}$  for lactose presented by compound **12** (Fig. 5e,f) and 1 mM for free lactose (Fig. 5g,h). An about 6-fold difference was determined in inhibitory potency of lactose presented by compound **9** and free lactose for galectin-1 (not shown), an about 100fold (50fold) difference between lactose presented by compound **9** (compound **12**) and free lactose for galectin-8 (Fig. 6a-d). In both cases, inhibitory potency appeared higher on lectin binding to tissue sections, between the synthetic compounds and lactose, than to the surface of the human tumor cells (Fig. 2d-f).

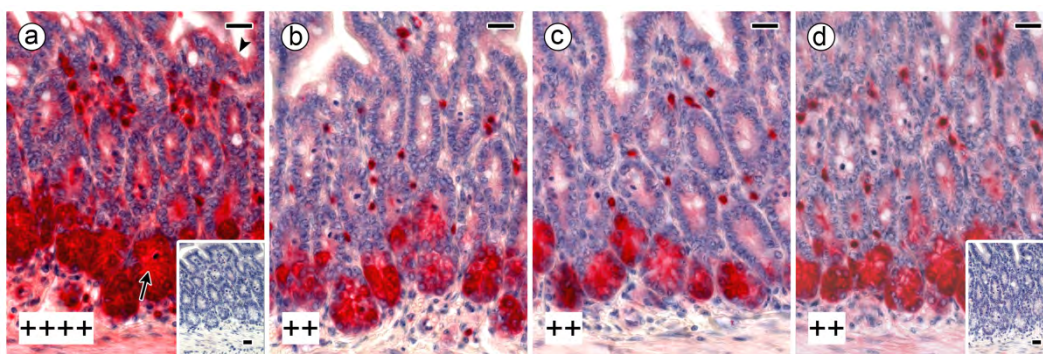


**Figure 6.** Illustration of galectin-8-dependent staining in sections of fixed murine jejunum in the absence of cognate sugar (100%-level: a; inset to a: negative control without labeled lectin) and its reduction to 50%-level by cognate sugar as free lactose (b) or presented by compounds **9** and **12**, respectively (c, d). Cytoplasm and striated border (arrowhead) of villi intestinales were stained by the lectin (0.33  $\mu\text{g}/\text{mL}$ ), even stronger signals were seen for epithelial cells of glandulae intestinales (arrow). Reduction to 50%-level was obtained in systematic titrations with 2.5 mM free lactose (b) as well as with 25  $\mu\text{M}$  sugar presented by compound **9** (c) and 50  $\mu\text{M}$  lactose presented by compound **12** (d), example for complete inhibition by 1 mM lactose presented by compound **12** given as inset to (d). Scale bars: 20  $\mu\text{m}$ .

These three assays thus report on the effect of the synthetic compounds on lectin binding to different ligands, i.e. on *N*-glycans of a glycoprotein, cell surface-presented glycans of cells adapted to growth in culture and glycans in sections of fixed tissues. As advantage of the histochemical assay, the monitoring of tissue sections even provides evidence for regional differences of signal reduction by free and compound-presented cognate sugar, seen in jejunum and galectin-3-dependent staining in favor of the synthetic products **9** and **12**. This observation underscores the potential of analyzing in parallel reduction of extent of positivity at diverse sites of an organ, represented in a section. For multifunctional effectors such as galectins, with counterreceptors in the glycocalyx such as laminin or fibronectin<sup>53-55</sup>, in the membrane such as integrins<sup>56</sup> and in the cytoplasm or nucleus such as bcl-2<sup>57, 58</sup>, respective information can be gleaned from a section, provided that tissue fixation did not harm reactivity. Moreover, considering a network of lectins, differential staining and reactivity patterns can be elucidated using the described protocol, as presented here for three human galectins.

### 3. Conclusions

This report extends the activity spectrum of thio-, disulfido- and selenogalactosides on a biohazard, i.e. a ricin-like toxin, to naphthalene-based disulfides and selenides presenting the cognate sugar galactose. The compounds had very little or no activity on human galectins, as already observed previously for mono-, bi- and trivalent disulfides attached to a benzene core

in *meta*-position.<sup>28</sup> Among the four thioglycosides and disulfides with lactose as ligand part, the naphthalene-based compound **9** proved most effective for galectins, with relative differences in potency depending on the structural design of the lectin. These results underline that a thiol-disulfide conversion, as exploited in works with dynamic combinatorial libraries<sup>18-20, 26</sup>, is an option for programming surface display and ligand density of glycodendrimersomes. These vesicle-like structures of adjustable architecture are versatile tools for measuring activity of galectins and other biomedically relevant lectins as intercellular glue.<sup>59-62</sup>

As part of soluble glycoclusters, involvement of *S*, *Se* atoms in the glycosidic bond confers distinct stereotopic and flexibility features to the sugar headgroup presentation. Its activity as lectin inhibitor is readily determined in a solid-phase assay (or related procedures; for compilation of methods, please see <sup>63</sup>). Considering a perspective for biomedical applications, thorough inspection of an impact on lectin binding to physiological counterreceptors and of cross-reactivity among related sugar receptors then are the arising challenges to be adequately addressed. The histochemical protocol applied herein can take respective studies another step forward to the envisioned aim.

## **4. Experimental**

### **4.1. Chemistry**

#### **4.1.1. General chemistry**

1,4-, 1,5-, 2,6-Bis(bromomethyl)naphthalenes and 1,3-, 1,4-bis(bromomethyl)benzenes were commercial products, 2,3,4,6-tetra-*O*-acetyl- $\beta$ -D-galactopyranosyl *isose*lenuonium bromide<sup>26</sup>, 1-thio-2,3,4,6-tetra-*O*-acetyl- $\beta$ -D-galactopyranose<sup>32, 33</sup> and 1-thio-2,3,6-tri-*O*-acetyl-4-(2,3,4,6-tetra-*O*-acetyl- $\beta$ -D-galactopyranosyl)- $\beta$ -D-glucopyranose<sup>34</sup> were prepared according to literature procedures. NMR spectra were recorded on a Bruker Avance II 500 (500/125 MHz for <sup>1</sup>H/<sup>13</sup>C) spectrometer. Chemical shifts are referenced to internal TMS (<sup>1</sup>H), or to the residual solvent signals (<sup>13</sup>C). Mass spectra were measured using a Bruker micrOTOFQ mass spectrometer. TLC was performed on DC-Alurolle Kieselgel F254 (Merck), and the compounds on the plates were visualized under UV light and by heating. For column chromatography, Kieselgel 60 (Merck, particle size 0.063-0.200) was used.

#### **4.1.2. General procedure for the preparation of thioglycosides (3,12)**

1,4-Bis(bromomethyl)naphthalene was dissolved in DMF at r.t. stirring under nitrogen atmosphere, then the peracetylated glycosylthiol was added, followed by triethylamine. Stirring was continued at r.t. until TLC indicated complete conversion of the starting materials (30 min) to products, then the reaction mixture was poured into water. A solid deposited which was filtered, rinsed with 3x10 mL water, and dried, yielding crude peracetylated products. The crude products were dissolved in methanol, stoichiometric amounts of LiOH.H<sub>2</sub>O added for deacetylation at 0 °C. The reaction mixture was allowed to warm to r.t. and when the starting material had completely reacted (TLC), the pH was adjusted to neutral by cation exchange resin, the suspension filtered, and the filtrate evaporated to dryness. The residue was stirred in acetone for 30 minutes, filtered, washed with acetone and dried to yield the 1,4-bis(bromomethyl)naphthalene-based thioglycosides.

#### 4.1.3. 1,4-Bis{1-[(β-D-galactopyranosyl)thio]methyl}naphthalene (3)

From 1,4-bis(bromomethyl)naphthalene (140 mg, 0.44 mmol), 2,3,4,6-tetra-*O*-acetyl-1-thio-β-D-galactopyranose (324.9 mg, 0.89 mmol) and triethylamine (0.1 mL, 1.36 mmol) 340 mg (87 %) of crude peracetylated **3** were obtained. Deacetylation as described above produced 56.4 mg (61 %) of **3**.  $[\alpha]_D^{22} -243$  (c 0.12 DMSO); <sup>1</sup>H NMR (CD<sub>3</sub>OD-DMSO-*d*<sub>6</sub>, 500 MHz): δ 8.23 (m, 2H, (H-5, H-8)<sup>Napht</sup>); 7.57 (m, 2H, (H-6, H-7)<sup>Napht</sup>); 7.39 (s, 2H, (H-2, H-3)<sup>Napht</sup>); 4.46 (d, 2H, CH<sub>2a</sub>, *J*<sub>a,b</sub> 13 Hz); 4.38 (d, 2H, CH<sub>2b</sub>); 4.25 (d, 2H, H-1,1'<sup>Gal</sup>, *J*<sub>1,2</sub> 9.7 Hz); 3.89 (d, 2H, H-4,4'<sup>Gal</sup>, *J*<sub>3,4</sub> 2.7 Hz); 3.83 (dd, 2H, H-6a,6a'<sup>Gal</sup>, *J*<sub>5,6a</sub> 7.0 Hz, *J*<sub>6a,6b</sub> 11.5 Hz); 3.75 (dd, 2H, H-6b,6b'<sup>Gal</sup>, *J*<sub>5,6b</sub> 5.1 Hz); 3.60 (dd, 2H, H-2,2'<sup>Gal</sup>, *J*<sub>2,3</sub> 9.4 Hz); 3.52 (m, 2H, H-5,5'); 3.38 (dd, 2H, H-3,3'<sup>Gal</sup>, *J*<sub>3,4</sub> 2.8 Hz, *J*<sub>2,3</sub> 9.2 Hz); <sup>13</sup>C NMR (DMSO, 125 MHz): δ 134.16 (C-1, C-4)<sup>Napht</sup>; 132.13 (C-1a, C-4a)<sup>Napht</sup>; 127.18 (C-2, C-3)<sup>Napht</sup>; 126.21 (C-6, C-7)<sup>Napht</sup>; 125.53 (C-5, C-8)<sup>Napht</sup>; 84.57 (C-1,1')<sup>Gal</sup>; 79.95 (C-5,5')<sup>Gal</sup>; 75.18 (C-3,3')<sup>Gal</sup>; 70.42 (C-2,2')<sup>Gal</sup>; 69.03 (C-4,4')<sup>Gal</sup>; 61.33 (C-6,6')<sup>Gal</sup>; 30.34 (CH<sub>2</sub>-S).

HRMS *m/z* Calcd for C<sub>24</sub>H<sub>32</sub>O<sub>10</sub>S<sub>2</sub> [M+Na]<sup>+</sup>: 567.133. Found: 567.134.

#### 4.1.4. 1,4-Bis{1-[(β-D-galactosyl-(1→4)-β-D-glucosyl)thio]methyl}naphthalene (12)

From 1,4-bis(bromomethyl)naphthalene (48.3 mg, 0.15 mmol), 1-thio-2,3,6-tri-*O*-acetyl-4-(2,3,4,6-tetra-*O*-acetyl-β-D-galactopyranosyl)-β-D-glucopyranose (201 mg, 0.31 mmol) and triethylamine (0.1 mL, 1.36 mmol) 168.3 mg (75 %) of crude **12** were obtained in peracetylated form. Deacetylation yielded 56.7 mg (63 %) of **12**.  $[\alpha]_D^{22} - 92$  (c 0.15 DMSO);

<sup>1</sup>H NMR (CD<sub>3</sub>OD, 500 MHz): δ 8.29 (m, 2H, (H-5, H-8)<sup>Napht</sup>); 7.57 (m, 2H, (H-6, H-7)<sup>Napht</sup>); 7.46 (s, 2H, (H-2, H-3)<sup>Napht</sup>); 4.49 (d, 2H, CH<sub>2a</sub>, *J*<sub>a,b</sub> 13.1 Hz); 4.38 (m, 4H, CH<sub>2b</sub>, H-1,1'<sup>Gal</sup> *J*<sub>1,2</sub> 7.7 Hz); 4.27 (d, 2H, H-1,1'<sup>Glc</sup>, *J*<sub>1,2</sub> 9.8 Hz); 3.95 (dd, 2H, H-6,6'<sup>aGlc</sup>, *J*<sub>6a,6b</sub> 12.2 Hz, *J*<sub>5,6a</sub> 2.6 Hz); 3.86 (dd, 2H, H-6,6'<sup>bGlc</sup>, *J*<sub>5,6b</sub> 4.6 Hz); 3.83 (d, 2H, H-4,4'<sup>Gal</sup>, *J*<sub>3,4</sub> 3.2 Hz); 3.78 (dd, 2H, H-6,6'<sup>aGal</sup>, *J*<sub>6a,6b</sub> 11.5 Hz, *J*<sub>5,6a</sub> 3.9 Hz); 3.71 (dd, 2H, H-6,6'<sup>bGal</sup>, *J*<sub>5,6b</sub> 4.6 Hz); 3.59 (m, 6H, H-5,5'<sup>Gal</sup>, H-4,4'<sup>Glc</sup>, H-2,2'<sup>Glc</sup>); 3.50 (dd, 2H, H-3,3'<sup>Gal</sup>, *J*<sub>2,3</sub> 9.8 Hz, *J*<sub>3,4</sub> 3.2 Hz); 3.47 (m, 2H, H-5,5'<sup>Glc</sup>); 3.44 (t, 2H, H-3,3'<sup>Glc</sup>, *J*<sub>2,3</sub> = *J*<sub>3,4</sub> 8.9 Hz); 3.34 (2H, H-2,2'<sup>Gal</sup>); <sup>13</sup>C NMR (DMSO-*d*<sub>6</sub>, 125 MHz): δ 133.95 (C-1, C-4)<sup>Napht</sup>; 132.12 (C-1a, C-4a)<sup>Napht</sup>; 127.26 (C-2, C-3)<sup>Napht</sup>; 126.27 (C-6, C-7)<sup>Napht</sup>; 125.56 (C-5, C-8)<sup>Napht</sup>; 104.34 (C-1,1')<sup>Gal</sup>; 83.69 (C-1,1')<sup>Glc</sup>; 81.35 (C-5,5')<sup>Glc</sup>; 79.67 (C-4,4')<sup>Glc</sup>; 76.93 (C-2,2')<sup>Gal</sup>; 75.98 (C-5,5')<sup>Gal</sup>; 73.71 (C-3,3')<sup>Gal</sup>; 73.31 (C-3,3')<sup>Glc</sup>; 71.00 (C-2,2')<sup>Glc</sup>; 68.61 (C-4,4')<sup>Gal</sup>; 61.25 (C-6,6')<sup>Gal</sup>; 60.86 (C-6,6')<sup>Glc</sup>; 30.32 (CH<sub>2</sub>-S).

HRMS *m/z* Calcd for C<sub>36</sub>H<sub>52</sub>O<sub>20</sub>S<sub>2</sub> [M+Na]<sup>+</sup>: 891.239. Found: 891.236.

#### 4.1.5. General procedure for the preparation of glycosyl disulfides (1,2,9,10,11)

Bis(methanesulfonylthiomethyl)arenes (B) were dissolved in 3 mL DMF at r.t. stirring under nitrogen atmosphere, peracetylated glycosylthiols were added, followed by triethylamine. Stirring was continued at r.t. until TLC indicated disappearance of the starting materials (30 min), then processed as described in 4.1.2.

#### 4.1.6. 1,5-Bis{1-[(β-D-galactopyranosyl)dithio]methyl}naphthalene (1)

From 1,5-bis(methanesulfonylthiomethyl)naphthalene (95.1 mg, 0.25 mmol), 1-thio-2,3,4,6-tetra-*O*-acetyl-β-D-galactopyranose (184.0 mg, 0.50 mmol) and triethylamine (0.1 mL, 1.36 mmol) 177 mg (74 %) of crude peracetylated **1** were obtained. Deacetylation yielded 68.9 mg (71 %) of **1**. [α]<sub>D</sub><sup>22</sup> – 40 (c 0.19 DMSO); <sup>1</sup>H NMR (CD<sub>3</sub>OD, 500 MHz): δ 8.25 (d, 2H, (H-4, H-8)<sup>Napht</sup>); 7.53 (d, 2H, (H-2, H-6)<sup>Napht</sup>); 7.49 (t, 2H, (H-3, H-7)<sup>Napht</sup>); 4.67 (d, 2H, CH<sub>2a</sub>) 4.57 (d, 2H, CH<sub>2b</sub> *J*<sub>a,b</sub> 10 Hz); 4.34 (d, 2H, H-1,1'<sup>Gal</sup>, *J*<sub>1,2</sub> 9.8 Hz); 3.94 (m, 4H, H-4,4'<sup>Gal</sup>, H-6a,6a'<sup>Gal</sup>); 3.81 (m, 4H, H-6b,6b'<sup>Gal</sup>, H-2,2'<sup>Gal</sup>); 3.59 (m, 2H, H-5,5'<sup>Gal</sup>); 3.53 (m, 2H, H-3,3'<sup>Gal</sup>); <sup>13</sup>C NMR (DMSO-*d*<sub>6</sub>, 125 MHz): δ 133.68 (C-1, C-5)<sup>Napht</sup>; 132.00 (C-1a, C-4a)<sup>Napht</sup>; 128.93 (C-2, C-6)<sup>Napht</sup>; 126.22 (C-3, C-7)<sup>Napht</sup>; 125.35 (C-8, C-4)<sup>Napht</sup>; 91.97 (C-1,1')<sup>Gal</sup>; 80.27 (C-5,5')<sup>Gal</sup>; 75.09 (C-3,3')<sup>Gal</sup>; 68.96 (C-2,2')<sup>Gal</sup>; 68.76 (C-4,4')<sup>Gal</sup>; 61.39 (C-6,6')<sup>Gal</sup>; 42.24 (CH<sub>2</sub>-S).

HRMS *m/z* Calcd for C<sub>24</sub>H<sub>32</sub>O<sub>10</sub>S<sub>4</sub> [M+Na]<sup>+</sup>: 631.078. Found: 631.073.

#### 4.1.7. 1,4-Bis{1-[( $\beta$ -D-galactopyranosyl)dithio]methyl}naphthalene (2)

From 1,4-bis(methanesulfonylthiomethyl)naphthalene (206.8 mg, 0.55 mmol), 1-thio-2,3,4,6-tetra-*O*-acetyl- $\beta$ -D-galactopyranose (400.0 mg, 1.10 mmol) and triethylamine (0.4 mL, 5.45 mmol) 406 mg (78 %) of crude peracetylated **2** were generated. Deacetylation yielded 55.9 mg (58 %) of **2**.  $[\alpha]_D^{22} - 64$  (c 0.16 DMSO);  $^1\text{H NMR}$  ( $\text{CD}_3\text{OD-DMSO-}d_6$ , 500 MHz):  $\delta$  8.34 (m, 2H, (H-5, H-8)<sup>Napht</sup>); 7.62 (m, 2H, (H-6, H-7)<sup>Napht</sup>); 7.50 (s, 2H, (H-2, H-3)<sup>Napht</sup>); 4.65 (d, 2H, CH<sub>2a</sub>) 4.55 (d, 2H, CH<sub>2b</sub>  $J_{a,b}$  10 Hz); 4.35 (d, 2H, H-1,1'<sup>Gal</sup>,  $J_{1,2}$  9.8 Hz); 3.97 (dd, 2H, H-4,4'<sup>Gal</sup>,  $J_{3,4}$  3.2 Hz  $J_{4,5} \sim 1$  Hz); 3.82 (dd, 2H, H-6a,6a'<sup>Gal</sup>,  $J_{5,6a}$  7.2 Hz,  $J_{6a,6b}$  11.9 Hz); 3.86 (dd, 2H, H-6b,6b'<sup>Gal</sup>,  $J_{5,6b}$  5.1 Hz); 3.81 (t, 2H, H-2,2'<sup>Gal</sup>,  $J_{2,3} = J_{1,2}$  9.4 Hz); 3.64 (m, 2H, H-5,5'<sup>Gal</sup>); 3.57 (dd, 2H, H-3,3'<sup>Gal</sup>);  $^{13}\text{C NMR}$  (DMSO- $d_6$ , 125 MHz):  $\delta$  133.30 (C-1, C-4)<sup>Napht</sup>; 131.89 (C-1a, C-4a)<sup>Napht</sup>; 128.37 (C-2, C-3)<sup>Napht</sup>; 126.74 (C-6, C-7)<sup>Napht</sup>; 125.67 (C-5, C-8)<sup>Napht</sup>; 91.99 (C-1,1')<sup>Gal</sup>; 80.26 (C-5,5')<sup>Gal</sup>; 75.09 (C-3,3')<sup>Gal</sup>; 68.96 (C-2,2')<sup>Gal</sup>; 68.75 (C-4,4')<sup>Gal</sup>; 61.39 (C-6,6')<sup>Gal</sup>; 42.02 (CH<sub>2</sub>-S). HRMS  $m/z$  Calcd for C<sub>24</sub>H<sub>32</sub>O<sub>10</sub>S<sub>4</sub> [M+Na]<sup>+</sup>: 631.078. Found: 631.075.

#### 4.1.8. 1,4-Bis{1-[( $\beta$ -D-galactosyl-(1 $\rightarrow$ 4)- $\beta$ -D-glucosyl)dithio]methyl}naphthalene (9)

586.1 mg (70 %) of crude peracetylated **9** were produced from 1,4-bis(methanesulfonylthiomethyl)naphthalene (206.8 mg, 0.55 mmol), 1-thio-2,3,6-tri-*O*-acetyl-4-(2,3,4,6-tetra-*O*-acetyl- $\beta$ -D-galactopyranosyl)- $\beta$ -D-glucopyranose (717.0 mg, 1.10 mmol) and triethylamine (0.21 mL, 2.86 mmol). Deacetylation yielded 67.7 mg (75 %) of **9**.  $[\alpha]_D^{22} - 173$  (c 0.19 DMSO);  $^1\text{H NMR}$  ( $\text{CD}_3\text{OD}$ , 500 MHz):  $\delta$  8.25 (m, 2H, (H-5, H-8)<sup>Napht</sup>); 7.59 (m, 2H, (H-6, H-7)<sup>Napht</sup>); 7.46 (s, 2H, (H-2, H-3)<sup>Napht</sup>); 4.61 (d, 2H, CH<sub>2a</sub>) 4.56 (d, 2H, CH<sub>2b</sub>  $J_{a,b}$  12.2 Hz); 4.43 (d, 2H, H-1,1'<sup>Gal</sup>,  $J_{1,2}$  7.7 Hz); 4.34 (d, 2H, H-1,1'<sup>Glc</sup>,  $J_{1,2}$  9.4 Hz); 3.94 (dd, 2H, H-6a,6a'<sup>Glc</sup>,  $J_{6a,6b}$  12.2 Hz,  $J_{5,6a}$  2.1 Hz); 3.89 (dd, 2H, H-6b,6b'<sup>Glc</sup>,  $J_{5,6b}$  4.0 Hz); 3.83 (d, 2H, H-4,4'<sup>Gal</sup>,  $J_{3,4}$  2.5 Hz); 3.80 (d, 2H, H-6a,6a'<sup>Gal</sup>,  $J_{6a,6b}$  11.3 Hz); 3.72 (dd, 2H, H-6b,6b'<sup>Gal</sup>,  $J_{5,6b}$  4.5 Hz); 3.67 (m, 4H, H-4,4'<sup>Glc</sup>, H-2,2'<sup>Glc</sup>); 3.63 (m, 2H, H-5,5'<sup>Gal</sup>); 3.57 (m, 4H, H-3,3'<sup>Glc</sup>, H-2,2'<sup>Gal</sup>); 3.50 (dd, 2H, H-3,3'<sup>Gal</sup>,  $J_{2,3}$  9.7 Hz,  $J_{3,4}$  3.1 Hz); 3.42 (m, 2H, H-5,5'<sup>Glc</sup>);  $^{13}\text{C NMR}$  (DMSO- $d_6$ , 125 MHz):  $\delta$  133.30 (C-1, C-4)<sup>Napht</sup>; 131.82 (C-1a, C-4a)<sup>Napht</sup>; 128.46 (C-2, C-3)<sup>Napht</sup>; 126.57 (C-6, C-7)<sup>Napht</sup>; 125.54 (C-5, C-8)<sup>Napht</sup>; 104.18 (C-1,1')<sup>Gal</sup>; 90.12 (C-1,1')<sup>Glc</sup>; 80.34 (C-5,5')<sup>Glc</sup>; 79.84 (C-4,4')<sup>Glc</sup>; 76.61 (C-2,2')<sup>Gal</sup>; 76.07 (C-5,5')<sup>Gal</sup>; 73.73 (C-3,3')<sup>Gal</sup>; 71.42 (C-3,3')<sup>Glc</sup>; 71.02 (C-2,2')<sup>Glc</sup>; 68.66 (C-4,4')<sup>Gal</sup>; 61.00 (C-6,6')<sup>Gal</sup>; 60.92 (C-6,6')<sup>Glc</sup>; 41.72 (CH<sub>2</sub>-S).

HRMS  $m/z$  Calcd for  $C_{36}H_{52}O_{20}S_4 [M+Na]^+$ : 955.183. Found: 955.179.

#### 4.1.9. 1,4-Bis{1-[( $\beta$ -D-galactosyl-(1 $\rightarrow$ 4)- $\beta$ -D-glucosyl)dithio]methyl}benzene (**10**)

From 1,4-bis(methanesulfonylthiomethyl)benzene (179.3 mg, 0.55 mmol), 1-thio-2,3,6-tri-*O*-acetyl-4-(2,3,4,6-tetra-*O*-acetyl- $\beta$ -D-galactopyranosyl)- $\beta$ -D-glucopyranose (717.0 mg, 1.1 mmol) and triethylamine (0.21 mL, 2.86 mmol) 491.1 mg (61 %) of crude peracetylated **10** were obtained. Deacetylation yielded 59.3 mg (66 %) of **10**.  $[\alpha]_D^{22} - 5$  (c 0.13 DMSO);  $^1H$  NMR ( $CD_3OD$ , 500 MHz):  $\delta$  7.31 (s, 4H)<sup>Xyl</sup>; 4.44 (d, 2H,  $CH_{2a}$ ,  $J_{a,b}$  9.1 Hz); 4.38 (d, 2H, H-1,1'<sup>Gal</sup>,  $J_{1,2}$  7.7 Hz); 4.35 (d, 2H,  $CH_{2b}$ ); 4.30 (d, 2H, H-1,1'<sup>Glc</sup>,  $J_{1,2}$  9.3 Hz); 3.92 (d, 2H, H-6a,6a'<sup>Glc</sup>,  $J_{6a,6b}$  12.2 Hz); 3.84 (dd, 2H, H-6b,6b'<sup>Glc</sup>,  $J_{5,6b}$  4.2 Hz); 3.80 (s, 2H, H-4,4'<sup>Gal</sup>); 3.77 (d, 2H, H-6a,6a'<sup>Gal</sup>,  $J_{6a,6b}$  11.4 Hz); 3.70 (dd, 2H, H-6b,6b'<sup>Gal</sup>,  $J_{5,6b}$  4.7 Hz); 3.58 (m, 6H, H-4,4'<sup>Glc</sup>, H-2,2'<sup>Glc</sup>, H-5,5'<sup>Gal</sup>); 3.47 (m, 6H, H-3,3'<sup>Gal</sup>, H-3,3'<sup>Glc</sup>, H-2,2'<sup>Gal</sup>); 3.43 (m, 2H, H-5,5'<sup>Gal</sup>);  $^{13}C$  NMR ( $DMSO-d_6$ , 125 MHz):  $\delta$  136.85 (C-1, C-4)<sup>Xyl</sup>; 129.91 (C-2, C-3, C-5, C-6)<sup>Xyl</sup>; 104.19 (C-1,1'<sup>Gal</sup>); 90.11 (C-1,1'<sup>Glc</sup>); 80.55 (C-5,5'<sup>Glc</sup>); 79.67 (C-4,4'<sup>Glc</sup>); 76.61 (C-2,2'<sup>Gal</sup>); 76.01 (C-5,5'<sup>Gal</sup>); 73.73 (C-3,3'<sup>Gal</sup>); 71.55 (C-3,3'<sup>Glc</sup>); 71.01 (C-2,2'<sup>Glc</sup>); 68.62 (C-4,4'<sup>Gal</sup>); 61.01 (C-6,6'<sup>Gal</sup>); 60.89 (C-6,6'<sup>Glc</sup>); 43.31 ( $CH_2-S$ ).

HRMS  $m/z$  Calcd for  $C_{32}H_{50}O_{20}S_4 [M+Na]^+$ : 905.168. Found: 905.167 .

#### 4.1.10. 1,5-Bis{1-[( $\beta$ -D-galactosyl-(1 $\rightarrow$ 4)- $\beta$ -D-glucosyl)dithio]methyl}naphthalene (**11**)

The reaction mixture with 1,5-bis(methanesulfonylthiomethyl)naphthalene (110.1 mg, 0.29 mmol), 1-thio-2,3,6-tri-*O*-acetyl-4-(2,3,4,6-tetra-*O*-acetyl- $\beta$ -D-galactopyranosyl)- $\beta$ -D-glucopyranose (381.7 mg, 0.58 mmol) and triethylamine (0.1 mL, 1.36 mmol) let us reach a yield of 295.1 mg (66 %) of crude peracetylated **11**. 55.9 mg (58 %) of **11** was obtained after deacetylation.  $[\alpha]_D^{22} - 13$  (c 0.13 DMSO);  $^1H$  NMR ( $CD_3OD$ , 500 MHz):  $\delta$  8.21 (d, 2H, (H-4, H-8)<sup>Napht</sup>); 7.53 (d, 2H, (H-2, H-6)<sup>Napht</sup>); 7.49 (t, 2H, (H-3, H-7)<sup>Napht</sup>); 4.63 (d, 2H,  $CH_{2a}$ ) 4.57 (d, 2H,  $CH_{2b}$   $J_{a,b}$  12.1 Hz); 4.43 (d, 2H, H-1,1'<sup>Gal</sup>,  $J_{1,2}$  7.6 Hz); 4.34 (d, 2H, H-1,1'<sup>Glc</sup>,  $J_{1,2}$  9.4 Hz); 3.95 (dd, 2H, H-6a,6a'<sup>Glc</sup>,  $J_{6a,6b}$  12.2 Hz,  $J_{5,6a}$  2.0 Hz); 3.89 (dd, 2H, H-6b,6b'<sup>Glc</sup>,  $J_{5,6b}$  4.1 Hz); 3.83 (d, 2H, H-4,4'<sup>Gal</sup>,  $J_{3,4}$  2.5 Hz); 3.81 (d, 2H, H-6a,6a'<sup>Gal</sup>,  $J_{6a,6b}$  11.3 Hz); 3.72 (dd, 2H, H-6b,6b'<sup>Gal</sup>,  $J_{5,6b}$  4.5 Hz); 3.68 (m, 4H, H-4,4'<sup>Glc</sup>, H-2,2'<sup>Glc</sup>); 3.63 (m, 2H, H-5,5'<sup>Gal</sup>); 3.57 (m, 4H, H-3,3'<sup>Glc</sup>, H-2,2'<sup>Gal</sup>); 3.50 (dd, 2H, H-3,3'<sup>Gal</sup>,  $J_{2,3}$  9.75 Hz); 3.43 (m, 2H, H-5,5'<sup>Glc</sup>);  $^{13}C$  NMR ( $DMSO-d_6$ , 125 MHz):  $\delta$  133.95 (C-1, C-5)<sup>Napht</sup>; 131.93 (C-1a, C-4a)<sup>Napht</sup>; 129.00 (C-2, C-6)<sup>Napht</sup>; 126.03 (C-3, C-7)<sup>Napht</sup>; 125.09 (C-8, C-4)<sup>Napht</sup>; 104.19 (C-1,1'<sup>Gal</sup>); 90.13 (C-1,1'<sup>Glc</sup>);

80.37 (C-5,5')<sup>Glc</sup>; 79.84 (C-4,4')<sup>Glc</sup>; 76.62 (C-2,2')<sup>Gal</sup>; 76.06 (C-5,5')<sup>Gal</sup>; 73.72 (C-3,3')<sup>Gal</sup>; 71.43 (C-3,3')<sup>Glc</sup>; 71.03 (C-2,2')<sup>Glc</sup>; 68.65 (C-4,4')<sup>Gal</sup>; 61.01 (C-6,6')<sup>Gal</sup>; 60.92 (C-6,6')<sup>Glc</sup>; 42.00 (CH<sub>2</sub>-S).

HRMS m/z Calcd for C<sub>35</sub>H<sub>50</sub>O<sub>20</sub>S<sub>4</sub> [M+Na]<sup>+</sup>: 955.183. Found: 955.181.

#### 4.1.11. General procedure for the preparation of selenoglycosides (4,5,6,7,8)

Bis(bromomethyl)arenes (A) were dissolved in DMF at r.t. stirring under nitrogen atmosphere, 2,3,4,6-tetra-*O*-acetyl-β-D-galactopyranosyl *iso*selenuronium bromide was added, followed by triethylamine. Stirring was continued at r.t. until TLC indicated consumption of the starting materials (30 min.) then the reaction mixture was poured into water (30 mL). The formed solid was filtered, rinsed with 3x10 mL water and dried, yielding crude peracetylated products. Deacetylation was effected as described under 4.1.2.

#### 4.1.12. 1,3-Bis{1-[(β-D-galactopyranosyl)seleno]methyl}benzene (4)

From 1,3-bis(bromomethyl)benzene (120 mg, 0.45 mmol), 2,3,4,6-tetra-*O*-acetyl-β-D-galactopyranosyl *iso*selenuronium bromide (486 mg, 0.91 mmol) and triethylamine (0.21 mL, 2.86 mmol) led to 421.8 mg (96 %) of crude peracetylated **4**. 75.0 mg (79 %) of **4** was obtained after deacetylation. [α]<sub>D</sub><sup>22</sup> –137 (c 0.17 DMSO); <sup>1</sup>H NMR (CD<sub>3</sub>OD-DMSO-*d*<sub>6</sub>, 500 MHz): δ 7.39 (m, 1H)<sup>Xyl</sup>; 7.21 (m, 3H)<sup>Xyl</sup>; 4.41 (d, 2H, H-1,1'<sup>Gal</sup>, *J*<sub>1,2</sub> 9.9 Hz); 4.12 (d, 2H, CH<sub>2a</sub>) 3.87 (d, 2H, CH<sub>2b</sub> *J*<sub>a,b</sub> 11.6 Hz); 3.89 (dd, 2H, H-4,4'<sup>Gal</sup>, *J*<sub>3,4</sub> 3.4 Hz *J*<sub>4,5</sub> 0.7 Hz); 3.84 (dd, 2H, H-6a,6a'<sup>Gal</sup>, *J*<sub>5,6a</sub> 7.1 Hz, *J*<sub>6a,6b</sub> 11.2 Hz); 3.74 (dd, 2H, H-6b,6b'<sup>Gal</sup>, *J*<sub>5,6b</sub> 5.0 Hz); 3.69 (t, 2H, H-2,2'<sup>Gal</sup>, *J*<sub>2,3</sub> = *J*<sub>1,2</sub> 9.2 Hz); 3.58 (m, 2H, H-5,5'<sup>Gal</sup>); 3.38 (dd, 2H, H-3,3'<sup>Gal</sup>); <sup>13</sup>C NMR (DMSO-*d*<sub>6</sub>, 125 MHz): δ 140.26 (C-1, C-3)<sup>Xyl</sup>; 129.93 (C-2)<sup>Xyl</sup>; 128.65 (C-5)<sup>Xyl</sup>; 127.34 (C-4, C-6)<sup>Xyl</sup>; 81.11 (C-1,1'<sup>Gal</sup>); 79.94 (C-5,5'<sup>Gal</sup>); 75.18 (C-3,3'<sup>Gal</sup>); 71.51 (C-2,2'<sup>Gal</sup>); 69.15 (C-4,4'<sup>Gal</sup>); 61.29 (C-6,6'<sup>Gal</sup>); 24.94 (CH<sub>2</sub>-Se).

HRMS m/z Calcd for C<sub>20</sub>H<sub>30</sub>O<sub>10</sub>Se<sub>2</sub> [M+Na]<sup>+</sup>: 613.007. Found: 613.007.

#### 4.1.13. 1,4-Bis{1-[(β-D-galactopyranosyl)seleno]methyl}benzene (5)

Starting with 1,4-bis(bromomethyl)benzene (120 mg, 0.45 mmol), 2,3,4,6-tetra-*O*-acetyl-β-D-galactopyranosyl *iso*selenuronium bromide (486 mg, 0.91 mmol) and triethylamine (0.21 mL, 2.86 mmol) 372 mg (88 %) of crude peracetylated **5** were synthesized. Deacetylation yielded 60.6 mg (64 %) of **5**. [α]<sub>D</sub><sup>22</sup> – 197 (c 0.15 DMSO); <sup>1</sup>H NMR (CD<sub>3</sub>OD-DMSO-*d*<sub>6</sub>, 500 MHz): δ

7.30 (s, 4H)<sup>Xyl</sup>; 4.46 (d, 2H, H-1,1'<sup>Gal</sup>,  $J_{1,2}$  9.8 Hz); 4.09 (d, 2H, CH<sub>2a</sub>) 3.91 (d, 2H, CH<sub>2b</sub>  $J_{a,b}$  11.6 Hz); 3.88 (dd, 2H, H-4,4'<sup>Gal</sup>,  $J_{3,4}$  3.5 Hz  $J_{4,5}$  ~1 Hz); 3.79 (dd, 2H, H-6a,6a'<sup>Gal</sup>,  $J_{5,6a}$  7.2 Hz,  $J_{6a,6b}$  11.6 Hz); 3.71 (dd, 2H, H-6b,6b'<sup>Gal</sup>,  $J_{5,6b}$  5.1 Hz); 3.67 (t, 2H, H-2,2'<sup>Gal</sup>,  $J_{2,3}=J_{1,2}$  9.2 Hz); 3.47 (m, 2H, H-5,5'<sup>Gal</sup>); 3.77 (dd, 2H, H-3,3'<sup>Gal</sup>); <sup>13</sup>C NMR (DMSO-*d*<sub>6</sub>, 125 MHz): δ 138.36 (C-1, C-4)<sup>Xyl</sup>; 129.27 (C-2, C-3, C-5, C-6)<sup>Xyl</sup>; 81.14 (C-1,1')<sup>Gal</sup>; 80.09 (C-5,5')<sup>Gal</sup>; 75.16 (C-3,3')<sup>Gal</sup>; 71.54 (C-2,2')<sup>Gal</sup>; 69.08 (C-4,4')<sup>Gal</sup>; 61.21 (C-6,6')<sup>Gal</sup>; 24.83 (CH<sub>2</sub>-Se). HRMS m/z Calcd for C<sub>20</sub>H<sub>30</sub>O<sub>10</sub>Se<sub>2</sub> [M+Na]<sup>+</sup>: 613.007. Found: 613.006.

#### 4.1.14. 2,6-Bis{1-[(β-D-galactopyranosyl)seleno]methyl}naphthalene (6)

From 2,6-bis(bromomethyl)naphthalene (120 mg, 0.38 mmol), 2,3,4,6-tetra-*O*-acetyl-β-D-galactopyranosyl *isoselenuronium* bromide (410 mg, 0.76 mmol) and triethylamine (0.21 mL, 2.86 mmol) 200 mg (54 %) of peracetylated **6** were obtained. Deacetylation yielded 67.6 mg (69 %) of **6**. [ $\alpha$ ]<sub>D</sub><sup>22</sup> – 201 (c 0.14 DMSO); <sup>1</sup>H NMR (CD<sub>3</sub>OD-DMSO-*d*<sub>6</sub>, 500 MHz): δ 7.65 (s, 2H, (H-1, H-5)<sup>Napht</sup>); 7.64 (d, 2H, (H-4, H-8)<sup>Napht</sup>); 7.39 (dd, 2H, (H-3, H-7)<sup>Napht</sup>); 4.29 (d, 2H, H-1,1'<sup>Gal</sup>,  $J_{1,2}$  9.8 Hz); 4.16 (d, 2H, CH<sub>2a</sub>) 3.92 (d, 2H, CH<sub>2b</sub>  $J_{a,b}$  11.8 Hz); 3.75 (dd, 2H, H-4,4'<sup>Gal</sup>,  $J_{3,4}$  3.3 Hz  $J_{4,5}$  ~1 Hz); 3.71 (dd, 2H, H-6a,6a'<sup>Gal</sup>,  $J_{5,6a}$  7.2 Hz,  $J_{6a,6b}$  11.9 Hz); 3.61 (dd, 2H, H-6b,6b'<sup>Gal</sup>,  $J_{5,6b}$  5.1 Hz); 3.57 (t, 2H, H-2,2'<sup>Gal</sup>,  $J_{2,3}=J_{1,2}$  9.8 Hz); 3.33 (m, 2H, H-5,5'<sup>Gal</sup>); 3.20 (dd, 2H, H-3,3'<sup>Gal</sup>); <sup>13</sup>C NMR (DMSO-*d*<sub>6</sub>, 125 MHz): δ 137.41 (C-2, C-6)<sup>Napht</sup>; 132.10 (C-1a, C-4a)<sup>Napht</sup>; 128.35 (C-4, C-8)<sup>Napht</sup>; 127.98 (C-3, C-7)<sup>Napht</sup>; 127.09 (C-1, C-5)<sup>Napht</sup>; 81.38 (C-1,1')<sup>Gal</sup>; 79.80 (C-5,5')<sup>Gal</sup>; 75.17 (C-3,3')<sup>Gal</sup>; 71.49 (C-2,2')<sup>Gal</sup>; 69.22 (C-4,4')<sup>Gal</sup>; 61.47 (C-6,6')<sup>Gal</sup>; 25.28 (CH<sub>2</sub>-Se).

HRMS m/z Calcd for C<sub>24</sub>H<sub>32</sub>O<sub>10</sub>Se [M+Na]<sup>+</sup>: 663.022. Found: 663.024.

#### 4.1.15. 1,4-Bis{1-[(β-D-galactopyranosyl)seleno]methyl}naphthalene (7)

From 1,4-bis(bromomethyl)naphthalene (240 mg, 0.76 mmol), 2,3,4,6-tetra-*O*-acetyl-β-D-galactopyranosyl *isoselenuronium* bromide (820 mg, 1.53 mmol) and triethylamine (0.4 mL, 5.45 mmol) 557 mg (75 %) of crude peracetylated **7** were produced. 82.1 mg (84 %) of **7** was obtained after deacetylation. [ $\alpha$ ]<sub>D</sub><sup>22</sup> – 271 (c 0.12 DMSO); <sup>1</sup>H NMR (CD<sub>3</sub>OD-DMSO-*d*<sub>6</sub>, 500 MHz): δ 8.22 (m, 2H)<sup>Napht</sup>; 7.57 (m, 2H)<sup>Napht</sup>; 7.37 (s, 2H)<sup>Napht</sup>; 4.40 (d, 2H, H-1,1'<sup>Gal</sup>,  $J_{1,2}$  9.8 Hz); 4.41 (d, 2H, CH<sub>2a</sub>); 4.30 (d, 2H, CH<sub>2b</sub>  $J_{a,b}$  11.9 Hz); 3.77 (dd, 2H, H-4,4'<sup>Gal</sup>,  $J_{3,4}$  3.2 Hz  $J_{4,5}$  ~1 Hz); 3.71 (dd, 2H, H-6a,6a'<sup>Gal</sup>,  $J_{5,6a}$  7.2 Hz,  $J_{6a,6b}$  11.9 Hz); 3.62 (dd, 2H, H-6b,6b'<sup>Gal</sup>,  $J_{5,6b}$  5.1 Hz); 3.56 (t, 2H, H-2,2'<sup>Gal</sup>,  $J_{2,3}$  = 9.4 Hz); 3.40 (m, 2H, H-5,5'<sup>Gal</sup>); 3.24 (dd, 2H, H-3,3'<sup>Gal</sup>); <sup>13</sup>C NMR (DMSO-*d*<sub>6</sub>, 125 MHz): δ 135.19 (C-1, C-4)<sup>Napht</sup>; 131.94 (C-1a, C-4a)<sup>Napht</sup>;

126.82 (C-2, C-3)<sup>Napht</sup>; 126.07 (C-6, C-7)<sup>Napht</sup>; 125.52 (C-5, C-8)<sup>Napht</sup>; 81.29 (C-1,1')<sup>Gal</sup>; 80.62 (C-5,5')<sup>Gal</sup>; 75.18 (C-3,3')<sup>Gal</sup>; 71.51 (C-2,2')<sup>Gal</sup>; 69.14 (C-4,4')<sup>Gal</sup>; 61.34 (C-6,6')<sup>Gal</sup>; 22.58 (CH<sub>2</sub>-Se).

HRMS m/z Calcd for C<sub>24</sub>H<sub>32</sub>O<sub>10</sub>Se [M+Na]<sup>+</sup>: 663.022. Found: 663.020.

#### 4.1.16. 1,5-Bis{1-[(β-D-galactopyranosyl)seleno]methyl}naphthalene (8)

From 1,5-bis(bromomethyl)naphthalene (240 mg, 0.76 mmol), 2,3,4,6-tetra-*O*-acetyl-β-D-galactopyranosyl isoselenuronium bromide (820 mg, 1.53 mmol) and triethylamine (0.4 mL, 5.45 mmol) a yield of 410 mg (55 %) of crude peracetylated **8** was reached. 88.6 mg (90 %) of **8** was obtained after deacetylation. [α]<sub>D</sub><sup>22</sup> – 321 (c 0.12 DMSO); <sup>1</sup>H NMR (CD<sub>3</sub>OD-DMSO-*d*<sub>6</sub>, 500 MHz): δ 8.19 (d, 2H, (H-4, H-8)<sup>Napht</sup>); 7.56 (d, 2H, (H-2, H-6)<sup>Napht</sup>); 7.50 (t, 2H, (H-3, H-7)<sup>Napht</sup>); 4.58 (d, 2H, CH<sub>2a</sub>); 4.56 (d, 2H, H-1,1'<sup>Gal</sup>, *J*<sub>1,2</sub> 9.8 Hz); 4.46 (d, 2H, CH<sub>2b</sub>, *J*<sub>a,b</sub> 11.9 Hz); 3.92 (dd, 2H, H-4,4'<sup>Gal</sup>, *J*<sub>3,4</sub> 3.3 Hz *J*<sub>4,5</sub> ~1 Hz); 3.86 (dd, 2H, H-6a,6a'<sup>Gal</sup>, *J*<sub>5,6a</sub> 7.0 Hz, *J*<sub>6a,6b</sub> 11.9 Hz); 3.77 (dd, 2H, H-6b,6b'<sup>Gal</sup>, *J*<sub>5,6b</sub> 5.2 Hz); 3.70 (t, 2H, H-2,2'<sup>Gal</sup>, *J*<sub>2,3</sub> = *J*<sub>1,2</sub>); 3.56 (m, 2H, H-5,5'<sup>Gal</sup>); 3.39 (dd, 2H, H-3,3'<sup>Gal</sup>); <sup>13</sup>C NMR (DMSO-*d*<sub>6</sub>, 125 MHz): δ 136.50 (C-1, C-5)<sup>Napht</sup>; 131.99 (C-1a, C-4a)<sup>Napht</sup>; 127.18 (C-2, C-6)<sup>Napht</sup>; 125.65 (C-3, C-7)<sup>Napht</sup>; 124.16 (C-8, C-4)<sup>Napht</sup>; 81.37 (C-1,1')<sup>Gal</sup>; 80.36 (C-5,5')<sup>Gal</sup>; 75.18 (C-3,3')<sup>Gal</sup>; 71.52 (C-2,2')<sup>Gal</sup>; 69.20 (C-4,4')<sup>Gal</sup>; 61.41 (C-6,6')<sup>Gal</sup>; 22.68 (CH<sub>2</sub>-Se).

HRMS m/z Calcd for C<sub>24</sub>H<sub>32</sub>O<sub>10</sub>Se [M+Na]<sup>+</sup>: 663.022. Found: 663.022.

## 4.2. Biochemistry

The plant toxin was obtained from dried mistletoe leaves, human galectins from recombinant production, then the proteins were purified from extracts by affinity chromatography as crucial step and rigorously controlled for purity by two-dimensional gel electrophoresis and mass spectrometry prior to labeling, as described.<sup>26, 28, 64, 65</sup> Matrix for binding of labeled lectin (VAA: 1,2 μg/mL; galectin-3: 3 μg/mL; galectin-8: 0.3 μg/mL) was established by adsorption of ASF (0.5 μg/50 μl) to the surface of microtiter plate wells and further processing with signal development by enzymatic reaction of sensor conjugate streptavidin/oxidase (Sigma, Munich, Germany) was performed as described in detail previously.<sup>26, 28</sup> In the cases of turbidity of solutions of the glycoconjugates in buffer, stock solutions were prepared in DMSO, as then also done for the controls.

## 4.3. Cell biology

Cells of the two human carcinoma line were grown and processed in FACScan analysis using the sensor conjugate streptavidin/R-phycoerythrin (Sigma) as described previously.<sup>26, 28</sup>

#### **4.4. Histochemistry**

Tissue specimen from four six-week-old C57BL/6 mice were fixed in Bouin's solution and processed to obtain sections (about 5 µm) as described.<sup>66-68</sup> Blocking of non-specific binding sites for proteins, specificity controls, the optimized staining protocol using biotinylated lectins and commercial kit reagents for signal development, documentation and semiquantitative assessment were carried out as described.<sup>67, 68</sup>

#### **Acknowledgements**

We gratefully acknowledge the excellent technical assistance by B. Hofer, inspiring discussions with Drs. B. Friday and A. Leddoz, the valuable comments of the reviewers as well as generous support by the Verein zur Förderung des biologisch-technologischen Fortschritts in der Medizin e.V. (Heidelberg, Germany). L. Sz. & K. F. thank the Hungarian Scientific Research Fund for the grant OTKA NN-109671. K. F. also acknowledges the support by a Marie Curie Career Integration Grant (303917 PGN-INNATE) and a grant from the Research Foundation-Flanders (1508414N and 1525517N). This research was furthermore supported by the EU and co-financed by the European Regional Development Fund under the project GINOP-2.3.2-15-2016-00008 (to L. Sz.).

#### **References**

1. Hakomori S-i. Aberrant glycosylation in tumors and tumor-associated carbohydrate antigens. *Adv Cancer Res.* 1989;52:257-331.
2. Cook GMW. Glycobiology of the cell surface: the emergence of sugars as an important feature of the cell periphery. *Glycobiology.* 1995;5:449-461.
3. Gabius H-J. The magic of the sugar code. *Trends Biochem Sci.* 2015;40:341.
4. Stowell SR, Ju T, Cummings RD. Protein glycosylation in cancer. *Annu Rev Pathol.* 2015;10:473-510.

5. Bhide GP, Colley KJ. Sialylation of *N*-glycans: mechanism, cellular compartmentalization and function. *Histochem Cell Biol.* 2017;147:149-174.
6. Corfield A. Eukaryotic protein glycosylation: a primer for histochemists and cell biologists. *Histochem Cell Biol.* 2017;147:119-147.
7. Caselitz J. Lectins and blood group substances as "tumor markers". *Curr Top Pathol.* 1987;77:245-277.
8. Gabius H-J, Manning JC, Kopitz J, André S, Kaltner H. Sweet complementarity: the functional pairing of glycans with lectins. *Cell Mol Life Sci.* 2016;73:1989-2016.
9. Gabius H-J, Roth J. An introduction to the sugar code. *Histochem Cell Biol.* 2017;147:111-117.
10. Varki A. Biological roles of glycans. *Glycobiology.* 2017;27:3-49.
11. Gabius H-J, Kaltner H, Kopitz J, André S. The glycobiology of the CD system: a dictionary for translating marker designations into glycan/lectin structure and function. *Trends Biochem Sci.* 2015;40:360-376.
12. Manning JC, Romero A, Habermann F, García Caballero G, Kaltner H, Gabius H-J. Lectins: a primer for histochemists and cell biologists. *Histochem Cell Biol.* 2017;147:199-222.
13. Roth J, Zuber C. Quality control of glycoprotein folding and ERAD: the role of *N*-glycan handling, EDEM1 and OS-9. *Histochem Cell Biol.* 2017;147:269-284.
14. Chabre YM, Roy R. The chemist's way to prepare multivalency. In: Gabius H-J, ed. *The Sugar Code. Fundamentals of glycosciences.* Weinheim, Germany: Wiley-VCH; 2009:53-70.
15. Chabre YM, Roy R. Design and creativity in synthesis of multivalent neoglycoconjugates. *Adv Carbohydr Chem Biochem.* 2010;63:165-393.
16. Roy R, Murphy PV, Gabius H-J. Multivalent carbohydrate-lectin interactions: how synthetic chemistry enables insights into nanometric recognition. *Molecules.* 2016;21:629.

17. Yue M, Han X, De Masi L, et al. Allelic variation contributes to bacterial host specificity. *Nat Commun.* 2015;6:8754.
18. Ramström O, Lehn J-M. In situ generation and screening of a dynamic combinatorial carbohydrate library against concanavalin A. *ChemBioChem.* 2000;1:41-48.
19. Ramström O, Lohmann S, Bunyapaiboonsri T, Lehn JM. Dynamic combinatorial carbohydrate libraries: probing the binding site of the concanavalin A lectin. *Chem Eur J.* 2004;10:1711-1715.
20. Sando S, Narita A, Aoyama Y. A facile route to dynamic glycopeptide libraries based on disulfide-linked sugar-peptide coupling. *Bioorg Med Chem Lett.* 2004;14:2835-2838.
21. Bernardes GJ, Grayson EJ, Thompson S, et al. From disulfide- to thioether-linked glycoproteins. *Angew Chem Int Ed.* 2008;47:2244-2247.
22. Szilágyi L, Illyés TZ, Herczegh P. Elaboration of a novel type of interglycosidic linkage: syntheses of disulfide disaccharides. *Tetrahedron Lett.* 2001;42:3901-3903.
23. Murthy BN, Sinha S, Surolia A, et al. Interactions of aromatic mannosyl disulfide derivatives with concanavalin A: synthesis, thermodynamic and NMR spectroscopy studies. *Carbohydr Res.* 2009;344:1758-1763.
24. Stellenboom N, Hunter R, Caira MR, Szilágyi L. A high-yielding, one-pot preparation of unsymmetrical glycosyl disulfides using 1-chlorobenzotriazole as an in situ trapping/oxidizing agent. *Tetrahedron Lett.* 2010;51:5309-5312.
25. Gutiérrez B, Muñoz C, Osorio L, et al. Aromatic glycosyl disulfide derivatives: evaluation of their inhibitory activities against *Trypanosoma cruzi*. *Bioorg Med Chem Lett.* 2013;23:3576-3579.
26. André S, Pei Z, Siebert H-C, Ramström O, Gabius H-J. Glycosyldisulfides from dynamic combinatorial libraries as O-glycoside mimetics for plant and mammalian lectins: their reactivities in solid-phase and cell assays and conformational analysis by molecular dynamics simulations. *Bioorg Med Chem.* 2006;14:6314-6323.

27. Martín-Santamaría S, André S, Buzamet E, et al. Symmetric dithiodigalactoside: strategic combination of binding studies and detection of selectivity between a plant toxin and human lectins. *Org Biomol Chem*. 2011;9:5445-5455.
28. André S, Kövér KE, Gabius H-J, Szilágyi L. Thio- and selenoglycosides as ligands for biomedically relevant lectins: valency-activity correlations for benzene-based dithiogalactoside clusters and first assessment for (di)selenodigalactosides. *Bioorg Med Chem Lett*. 2015;25:931-935.
29. Gabius H-J. Probing the cons and pros of lectin-induced immunomodulation: case studies for the mistletoe lectin and galectin-1. *Biochimie*. 2001;83:659-666.
30. Kaltner H, Toegel S, García Caballero G, Manning JC, Ledeen RW, Gabius H-J. Galectins: their network and roles in immunity/tumor growth control. *Histochem Cell Biol*. 2017;147:239-256.
31. Kumar AA, Illyés TZ, Kövér KE, Szilágyi L. Convenient syntheses of 1,2-trans selenoglycosides using isoselenuronium salts as glycosylselenenyl transfer reagents. *Carbohydr Res*. 2012;360:8-18.
32. Cerny M, Pacak J, Stanek J. 2,3,4,6-Tetra-*O*-acetyl- $\beta$ -D-galaktopyranosylmercaptan und dessen Anwendung zur Synthese von  $\beta$ -D-Thiogalaktosiden. *Monatsh Chem*. 1963;94:290-294.
33. Gamblin DP, Garnier P, van Kasteren S, Oldham NJ, Fairbanks AJ, Davis BG. Glyco-SeS: selenenylsulfide-mediated protein glycoconjugation: a new strategy in post-translational modification. *Angew Chem Int Ed*. 2004;43:828-833.
34. Stanek J, Sindlerová M, Cerny M. Derivatives of D-thioxylopyranose and of some reducing 1-deoxy-1-thiodisaccharides. *Collect Czech Chem Commun*. 1965;30:297-303.
35. Muñoz FJ, Santos JI, Ardá A, et al. Binding studies of adhesion/growth-regulatory galectins with glycoconjugates monitored by surface plasmon resonance and NMR spectroscopy. *Org Biomol Chem*. 2010;8:2986-2992.

36. Jiménez M, André S, Siebert H-C, Gabius H-J, Solís D. AB-type lectin (toxin/agglutinin) from mistletoe: differences in affinity of the two galactoside-binding Trp/Tyr-sites and regulation of their functionality by monomer/dimer equilibrium. *Glycobiology*. 2006;16:926-937.
37. Schwefel D, Maierhofer C, Beck JG, et al. Structural basis of multivalent binding to wheat germ agglutinin. *J Am Chem Soc*. 2010;132:8704-8719.
38. Rohse P, Wittmann V. Mechanistic insight into nanomolar binding of multivalent neoglycopeptides to wheat germ agglutinin. *Chem Eur J*. 2016;22:9724-9733.
39. Strino F, Lii JH, Koppisetty CA, Nyholm PG, Gabius H-J. Selenoglycosides in silico: *ab initio*-derived reparameterization of MM4, conformational analysis using histo-blood group ABH antigens and lectin docking as indication for potential of bioactivity. *J Comput Aided Mol Des*. 2010;24:1009-1021.
40. Gupta D, Kaltner H, Dong X, Gabius H-J, Brewer CF. Comparative cross-linking activities of lactose-specific plant and animal lectins and a natural lactose-binding immunoglobulin G fraction from human serum with asialofetuin. *Glycobiology*. 1996;6:843-849.
41. André S, Liu B, Gabius H-J, Roy R. First demonstration of differential inhibition of lectin binding by synthetic tri- and tetravalent glycoclusters from cross-coupling of rigidified 2-propynyl lactoside. *Org Biomol Chem*. 2003;1:3909-3916.
42. André S, Specker D, Bovin NV, et al. Carbamate-linked lactose: design of clusters and evidence for selectivity to block binding of human lectins to (neo)glycoproteins with increasing degree of branching and to tumor cells. *Bioconjugate Chem*. 2009;20:1716-1728.
43. André S, Lahmann M, Gabius H-J, Oscarson S. Glycocluster design for improved avidity and selectivity in blocking human lectin/plant toxin binding to glycoproteins and cells. *Mol Pharmaceut*. 2010;7:2270-2279.

44. Giguère D, André S, Bonin MA, et al. Inhibitory potential of chemical substitutions at bioinspired sites of  $\alpha$ -D-galactopyranose on neoglycoprotein/cell surface binding of two classes of medically relevant lectins. *Bioorg Med Chem*. 2011;19:3280-3287.
45. André S, Jarikote DV, Yan D, et al. Synthesis of bivalent lactosides and their activity as sensors for differences between lectins in inter- and intrafamily comparisons. *Bioorg Med Chem Lett*. 2012;22:313-318.
46. Smetana Jr K, André S, Kaltner H, Kopitz J, Gabius H-J. Context-dependent multifunctionality of galectin-1: a challenge for defining the lectin as therapeutic target. *Expert Opin Ther Targets*. 2013;17:379-392.
47. Campo VL, Marchiori MF, Rodrigues LC, Dias-Baruffi M. Synthetic glycoconjugates inhibitors of tumor-related galectin-3: an update. *Glycoconj J*. 2016;33:853-876.
48. Friedel M, André S, Goldschmidt H, Gabius H-J, Schwartz-Albiez R. Galectin-8 enhances adhesion of multiple myeloma cells to vascular endothelium and is an adverse prognostic factor. *Glycobiology*. 2016;26:1048-1058.
49. Toegel S, Bieder D, André S, et al. Human osteoarthritic knee cartilage: fingerprinting of adhesion/growth-regulatory galectins *in vitro* and *in situ* indicates differential upregulation in severe degeneration. *Histochem Cell Biol*. 2014;142:373-388.
50. Toegel S, Weinmann D, André S, et al. Galectin-1 couples glycobiology to inflammation in osteoarthritis through the activation of an NF- $\kappa$ B-regulated gene network. *J Immunol*. 2016;196:1910-1921.
51. Weinmann D, Schlangen K, André S, et al. Galectin-3 induces a pro-degradative/inflammatory gene signature in human chondrocytes, teaming up with galectin-1 in osteoarthritis pathogenesis. *Sci Rep*. 2016;6:39112.
52. Lohr M, Kaltner H, Schwartz-Albiez R, Sinowatz F, Gabius H-J. Towards functional glycomics by lectin histochemistry: strategic probe selection to monitor core and

- branch-end substitutions and detection of cell-type and regional selectivity in adult mouse testis and epididymis. *Anat Histol Embryol.* 2010;39:481-493.
53. Woo H-J, Shaw LM, Messier JM, Mercurio AM. The major non-integrin laminin-binding protein of macrophages is identical to carbohydrate-binding protein 35 (Mac-2). *J Biol Chem.* 1990;265:7097-7099.
54. Zhou Q, Cummings RD. L-14 lectin recognition of laminin and its promotion of *in vitro* cell adhesion. *Arch Biochem Biophys.* 1993;300:6-17.
55. Ohannesian DW, Lotan D, Thomas P, et al. Carcinoembryonic antigen and other glycoconjugates act as ligands for galectin-3 in human colon carcinoma cells. *Cancer Res.* 1995;55:2191-2199.
56. Amano M, Eriksson H, Manning JC, et al. Tumour suppressor p16<sup>INK4a</sup>: anoikis-favouring decrease in *N/O*-glycan/cell surface sialylation by down-regulation of enzymes in sialic acid biosynthesis in tandem in a pancreatic carcinoma model. *FEBS J.* 2012;279:4062-4080.
57. Liu F-T, Patterson RJ, Wang JL. Intracellular functions of galectins. *Biochim Biophys Acta.* 2002;1572:263-273.
58. Dawson H, André S, Karamitopoulou E, Zlobec I, Gabius H-J. The growing galectin network in colon cancer and clinical relevance of cytoplasmic galectin-3 reactivity. *Anticancer Res.* 2013;33:3053-3059.
59. Percec V, Leowanawat P, Sun HJ, et al. Modular synthesis of amphiphilic Janus glycodendrimers and their self-assembly into glycodendrimersomes and other complex architectures with bioactivity to biomedically relevant lectins. *J Am Chem Soc.* 2013;135:9055-9077.
60. Zhang S, Moussodia R-O, Murzeau C, et al. Dissecting molecular aspects of cell interactions using glycodendrimersomes with programmable glycan presentation and engineered human lectins. *Angew Chem Int Ed.* 2015;54:4036-4040.

61. Zhang S, Moussodia R-O, Vértesy S, et al. Unraveling functional significance of natural variations of a human galectin by glycodendrimersomes with programmable glycan surface. *Proc Natl Acad Sci USA*. 2015;112:5585-5590.
62. Xiao Q, Wang Z, Williams D, et al. Why do membranes of some unhealthy cells adopt a cubic architecture? *ACS Cent Sci*. 2016;2:943-953.
63. Solís D, Bovin NV, Davis AP, et al. A guide into glycosciences: how chemistry, biochemistry and biology cooperate to crack the sugar code. *Biochim Biophys Acta*. 2015;1850:186-235.
64. Gabius H-J, Walzel H, Joshi SS, et al. The immunomodulatory  $\beta$ -galactoside-specific lectin from mistletoe: partial sequence analysis, cell and tissue binding and impact on intracellular biosignaling of monocytic leukemia cells. *Anticancer Res*. 1992;12:669-676.
65. Vértesy S, Michalak M, Miller MC, et al. Structural significance of galectin design: impairment of homodimer stability by linker insertion and partial reversion by ligand presence. *Protein Eng Des Sel*. 2015;28:199-210.
66. Manning JC, Seyrek K, Kaltner H, André S, Sinowatz F, Gabius H-J. Glycomic profiling of developmental changes in bovine testis by lectin histochemistry and further analysis of the most prominent alteration on the level of the glycoproteome by lectin blotting and lectin affinity chromatography. *Histol Histopathol*. 2004;19:1043-1060.
67. André S, Kaltner H, Kayser K, Murphy PV, Gabius H-J. Merging carbohydrate chemistry with lectin histochemistry to study inhibition of lectin binding by glycoclusters in the natural tissue context. *Histochem Cell Biol*. 2016;145:185-199.
68. Roy R, Cao Y, Kaltner H, et al. Teaming up chemistry and histology for activity screening in galectin-directed inhibitor design. *Histochem Cell Biol*. 2017;147:285-301.

## Legends

**Chart 1** Structures of thio-, disulfido- and selenoglycoside derivatives **1-12**

**Chart 2** Syntheses of thio- and seleno derivatives **1-12**

**Figure 1.** Geometric parameters to define distances between and relative orientations of sugar units obtained by molecular dynamics simulations for **4** (a & b), **5** (c & d), **9** (e & f) and **11** (g & h). The plots depict changes of the separation between sugar units as defined by C1-C1' distance (in Å) of galactose units in **4** & **5** (a & c) and that of glucose residues of the lactose units in **9** & **11** (e & g) as a function of the pseudo torsion angles (in deg) as defined by GalC4-GalC1-GalC1'-GalC4' for **4** & **5** and by GalC4-GlcC1-GlcC1'-GalC4' for **9** & **11**, respectively, denoted as the “core dihedral”; as well as variations of the pseudo torsion angles defined by the GalC4-GalO4-GalC4'-GalO4' denoted as the “galactose dihedral” as a function of the core dihedrals for **4** & **5** (b & d) and for **9** & **11** (f & h).

**Figure 2.** Flow cytometric analysis of extent of inhibition of lectin binding to cell surface glycans (tested on the human colon adenocarcinoma line SW480 (a-c) and the pancreatic carcinoma line Capan-1 reconstituted for expression of the human tumor suppressor p16<sup>INK4a</sup> (d-f)) by cognate sugar, free or as part of bivalent glycoconjugates. Numbers in each panel give percentage of positive cells/mean fluorescence intensity, the grey curve represents the 0%-level (background control) in the absence of labeled lectin (set of numbers given on top of list in the right part of each illustration). VAA-dependent staining when increasing lectin concentration from 0.1 µg/mL to 0.2 µg/mL,

0.5  $\mu\text{g}/\text{mL}$ , 1  $\mu\text{g}/\text{mL}$  and 2  $\mu\text{g}/\text{mL}$  (a) and with lectin (2  $\mu\text{g}/\text{mL}$  fluorescent lectin) in the presence of 0.5 mM galactose presented by compound **2**, of 2 mM by compound **8** and of 0.5 mM by compound **3** as well as in the absence of cognate sugar (100%-level) (curves from left to right, numbers in list from top to bottom) (b). Galectin-3-dependent staining (10  $\mu\text{g}/\text{mL}$  biotinylated lectin) in the presence of 0.1 mM lactose presented by compound **9** and as free sugar as well as in the absence of sugar (c). Galectin-1-dependent staining (20  $\mu\text{g}/\text{mL}$  fluorescent lectin) in the presence of 10 mM free lactose and of 1 mM lactose presented by compounds **9** and **11**, respectively, as well as in the absence of sugar (d). Staining by the engineered galectin-1 variant with covalent connection of the two lectin domains (2  $\mu\text{g}/\text{mL}$  fluorescent lectin) in the presence of 2 mM lactose presented by compound **9**, 10 mM free lactose and 2 mM lactose presented by compound **11** as well as in the absence of sugar (e). Galectin-8-dependent staining (2  $\mu\text{g}/\text{mL}$  fluorescent lectin) in the presence of 2 mM lactose presented by compound **9** and 10 mM free lactose as well as in the absence of sugar (f).

**Figure 3.** Stepwise reduction of VAA-dependent staining in sections of fixed adult murine kidney by presence of increasing concentrations of cognate sugar (galactose). The lectin (at 1  $\mu\text{g}/\text{mL}$ ) bound strongly to epithelial lining and brush border of proximal tubules (P), whereas glomeruli (G) and distal tubules (D) remained mostly unstained. In titrations, the 100%-level of signal intensity was still obtained in the presence of 2 mM free galactose (a) and 0.1 mM of scaffold-presented galactose (by compound **2**: e; by compound **6**: i). Increases of sugar concentration (5 mM (b), 10 mM (c) and 50 mM (d) of free galactose; 0.5 mM (f, j), 1 mM (g, k) and 5 mM (h, l) galactose in disulfide **2** (e-h) and selenide **6** (i-l)) led to increasing degrees of inhibition of lectin binding. The corresponding category of signal intensity after semiquantitative grading is given in the bottom left part of each microphotograph, following intensity assessment according to

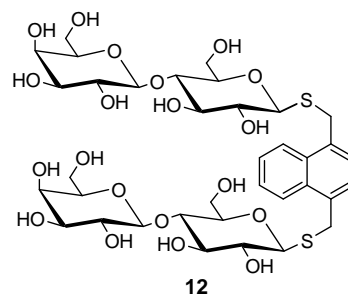
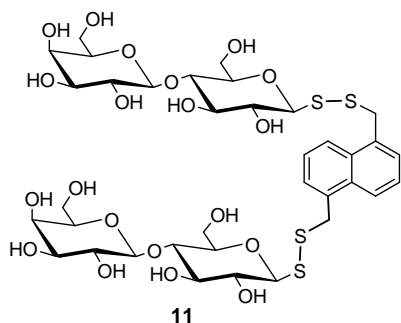
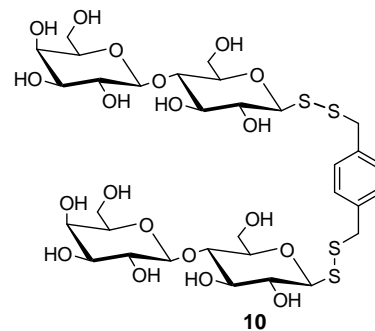
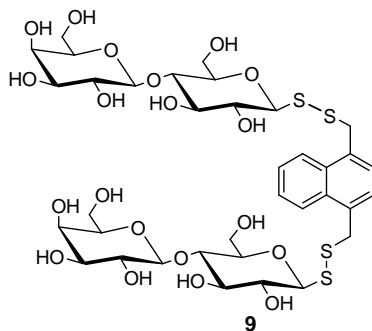
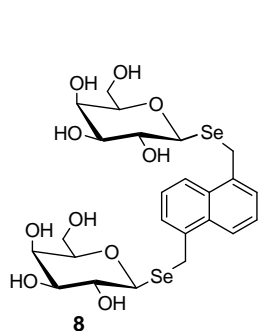
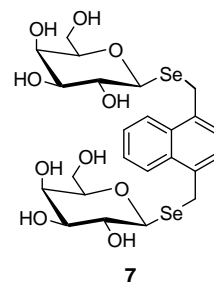
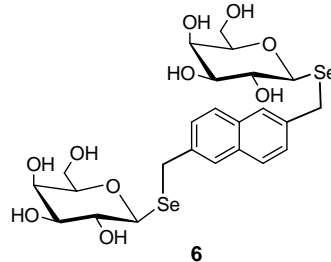
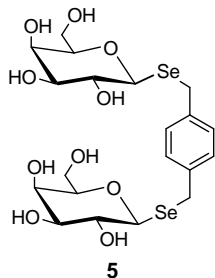
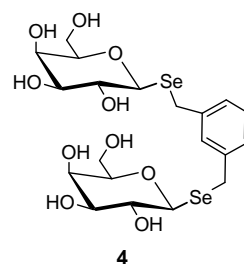
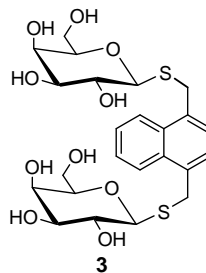
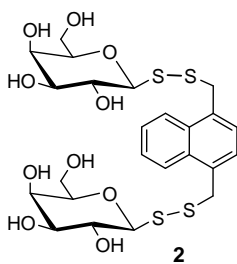
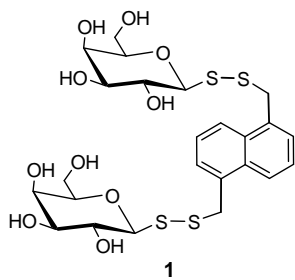
the following system: -, no staining; (+), very weak but significant staining; +, weak staining; ++, medium-level staining; +++, strong staining; +++++, very strong staining. Scale bars: 20  $\mu\text{m}$ .

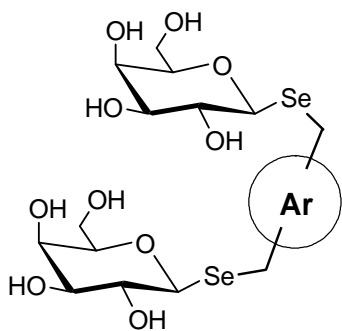
**Figure 4.** Stepwise reduction of VAA-dependent staining in sections of the corpus region of fixed murine epididymis (a-d) and of jejunum (e-h) by presence of increasing concentrations of cognate sugar (galactose). The lectin (at 1  $\mu\text{g}/\text{mL}$ ) bound strongly to the epithelial lining of ductus epididymidis, here especially in the supranuclear area of principal cells (arrow), also to stereocilia on the luminal surface of principal cells (arrowhead) and luminal spermatozoa (S), shown in a. In jejunum, shown in e, lamina propria mucosae of villi intestinales (L) and glandulae intestinales (arrow) were main sites of strong signal intensity. No reduction of signal intensity was seen in the presence of up to 1 mM free galactose (a, e). For the two organs, presence of 5 mM/10 mM free galactose (b/f), of 0.5 mM/1 mM galactose presented by compound **2** (c/g) or 0.25 mM/1 mM galactose presented by compound **6** (d/h) inhibited lectin binding by about 50%. Staining of the striated border and cytoplasm of the epithelial lining (arrowheads) appears less affected by lactose (f) than by the lactoside derivatives (g, h). Complete inhibition was obtained at 50 mM free galactose (insets to a, e) and at 10 mM of scaffold-presented galactose (insets to c, g and to d, h). Scale bars: 20  $\mu\text{m}$ .

**Figure 5.** Stepwise reduction of galectin-3-dependent staining in sections of fixed murine jejunum by presence of increasing concentrations of cognate sugar (lactose). The lectin (at 4  $\mu\text{g}/\text{mL}$ ) bound strongly to epithelial cells in glandulae intestinales (asterisk) and also to the apical part of epithelial cells in villi intestinales (arrow). Goblet cells, in contrast, were negative (arrowhead). Staining intensity remained at the 100%-level in the presence of up to 5  $\mu\text{M}$  lactose presented by compound **9** (a) and decreased when

increasing the sugar concentration to 10  $\mu$ M (b), 25  $\mu$ M (c) and 50  $\mu$ M (d). Testing the  $IC_{50}$  of lactose for this compound (at 25  $\mu$ M of lactose) presented by compound **12** (e) and for free lactose (g) revealed less (e) or no (g) effect. The concentration for reaching 50%-level was 50  $\mu$ M for the thioglycoside **12** (f) and 1 mM for free lactose (h). Scale bars: 20  $\mu$ m.

**Figure 6.** Illustration of galectin-8-dependent staining in sections of fixed murine jejunum in the absence of cognate sugar (100%-level: a; inset to a: negative control without labeled lectin) and its reduction to 50%-level by cognate sugar as free lactose (b) or presented by compounds **9** and **12**, respectively (c, d). Cytoplasm and striated border (arrowhead) of villi intestinales were stained by the lectin (0.33  $\mu$ g/mL), even stronger signals were seen for epithelial cells of glandulae intestinales (arrow). Reduction to 50%-level was obtained in systematic titrations with 2.5 mM free lactose (b) as well as with 25  $\mu$ M sugar presented by compound **9** (c) and 50  $\mu$ M lactose presented by compound **12** (d), example for complete inhibition by 1 mM lactose presented by compound **12** given as inset to (d). Scale bars: 20  $\mu$ m.





4 Ar: 1,3-xylyl

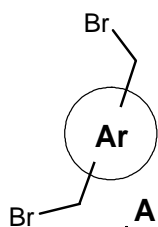
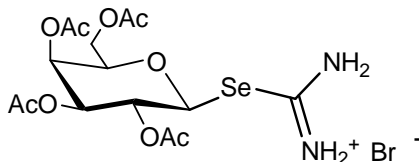
5 Ar: 1,4-xylyl

6 Ar: 2,6-naphthyl

7 Ar: 1,4-naphthyl

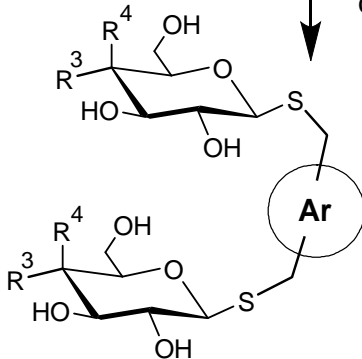
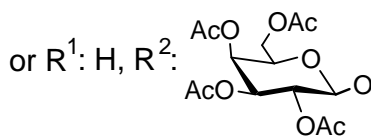
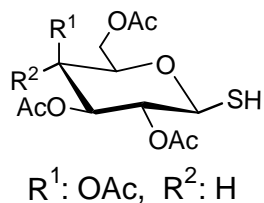
8 Ar: 1,5-naphthyl

a, b



A

a, b

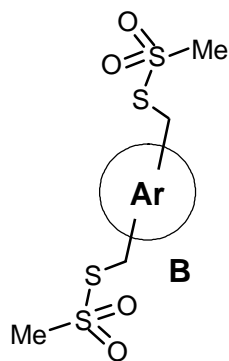


3 Ar: 1,4-naphthyl R<sup>3</sup>:H, R<sup>4</sup>:OH

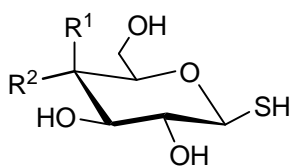
12 Ar: 1,4-naphthyl

R<sup>3</sup>: HO OH R<sup>4</sup>: H

Reaction conditions: (a) Et<sub>3</sub>N / DMF, rt; (b) LiOH / MeOH, rt

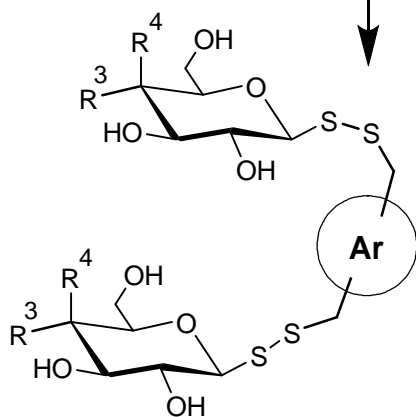
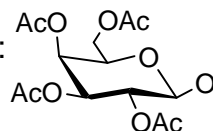


a, b



R<sup>1</sup>: OAc, R<sup>2</sup>: H

or R<sup>1</sup>: H, R<sup>2</sup>:



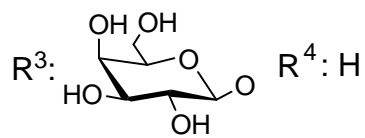
1 Ar: 1,5-naphthyl

R<sup>3</sup>: H; R<sup>4</sup>: OH

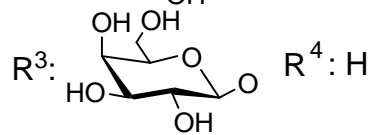
2 Ar: 1,4-naphthyl

R<sup>3</sup>: H; R<sup>4</sup>: OH

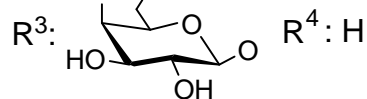
9 Ar: 1,4-naphthyl



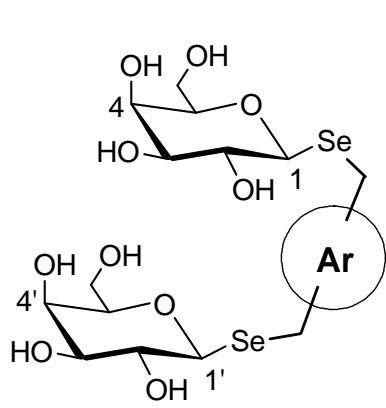
10 Ar: 1,4-xyllyl



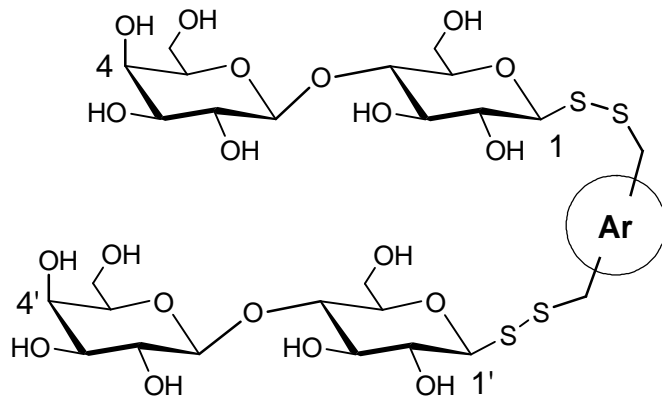
11 Ar: 1,5-naphthyl



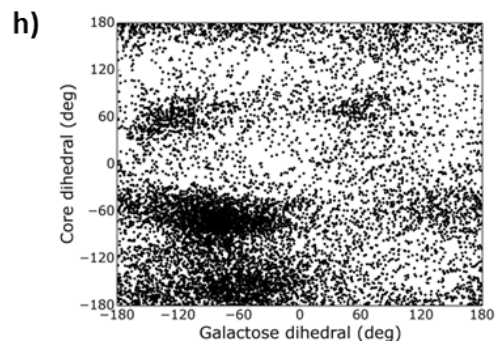
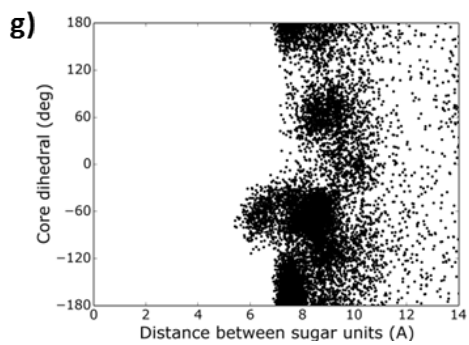
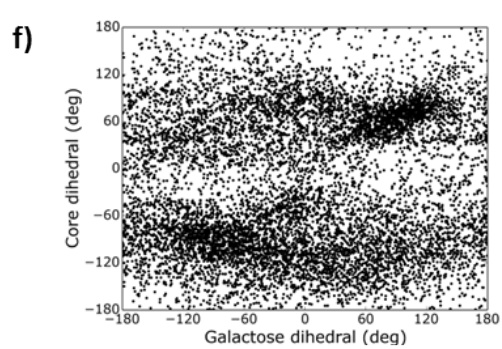
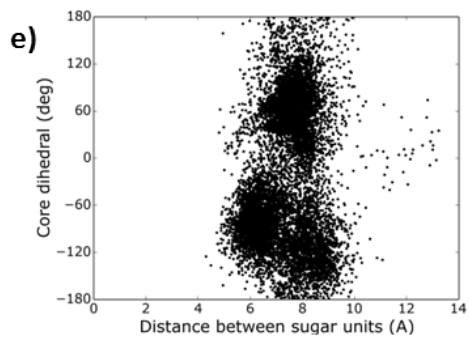
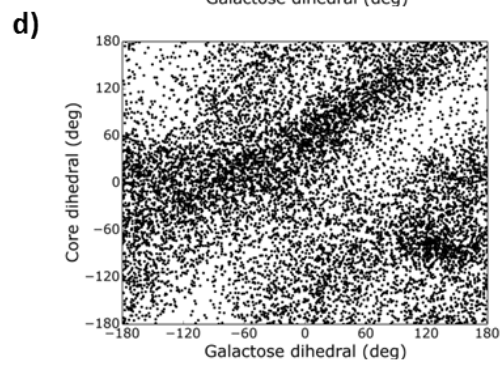
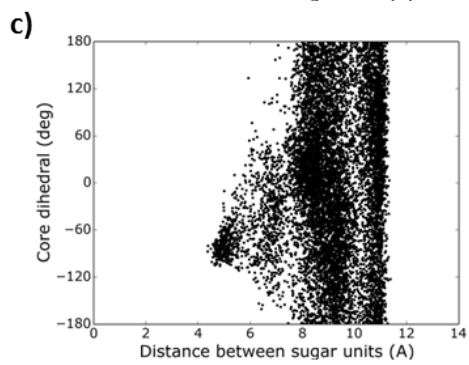
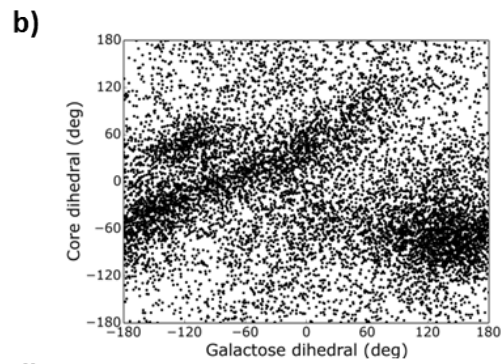
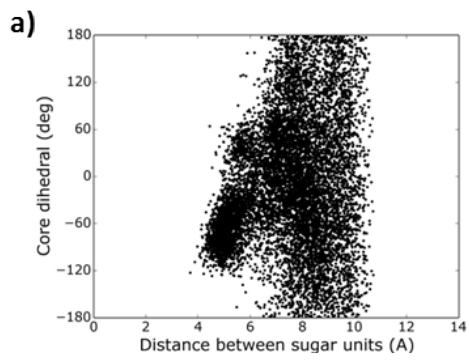
Reaction conditions: (a) Et<sub>3</sub>N / DMF, rt; (b) LiOH / MeOH, rt

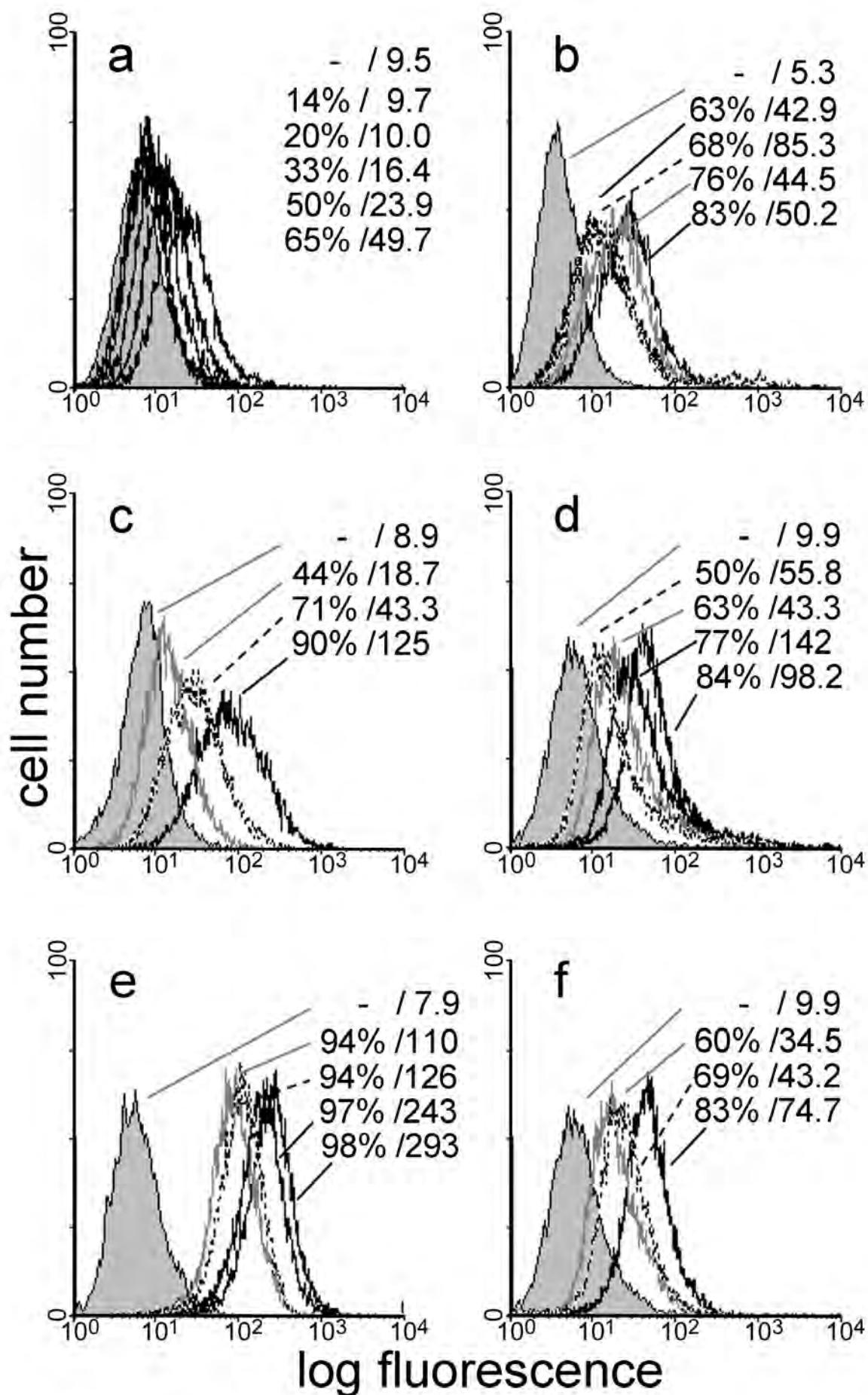


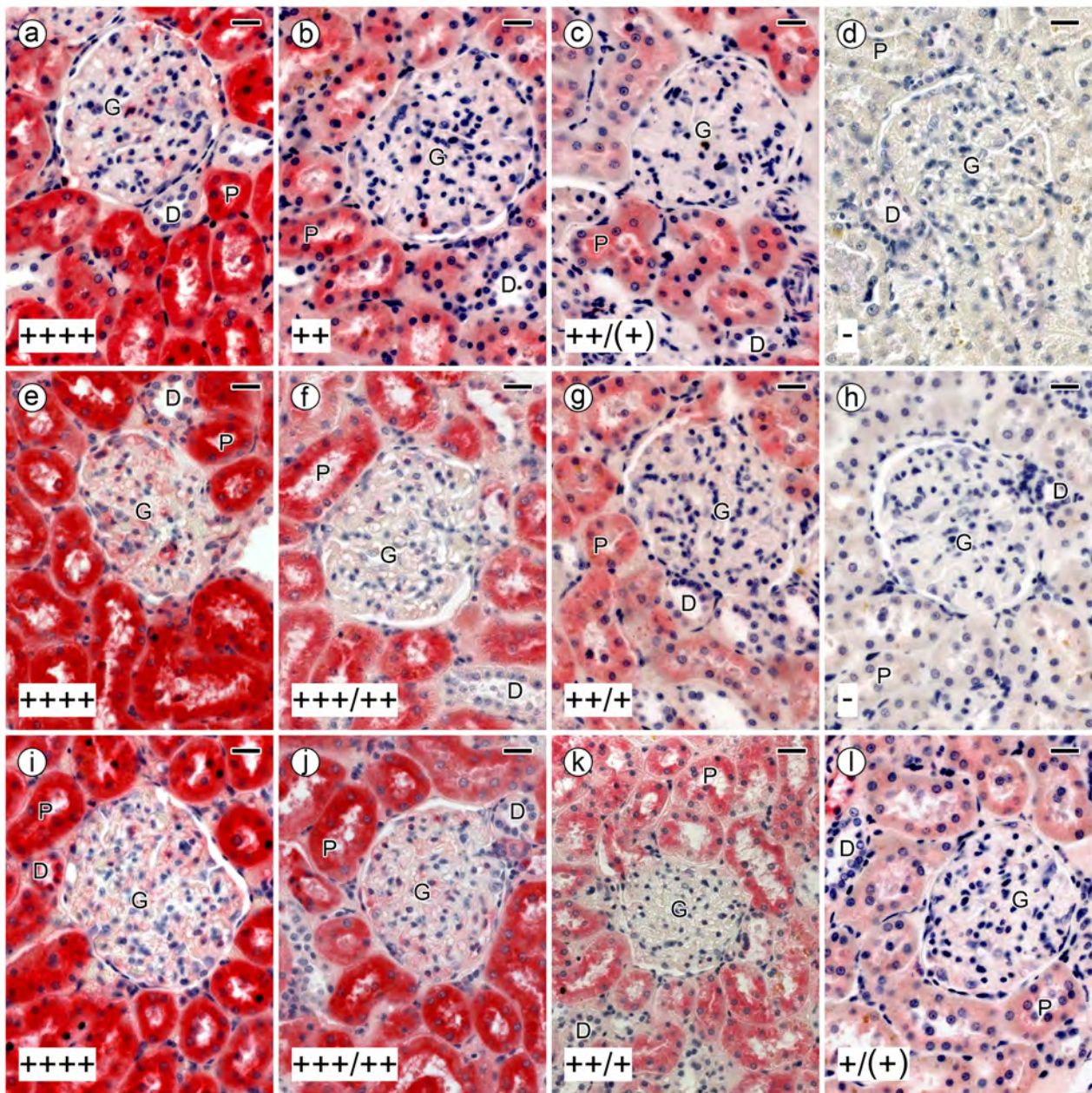
4, 5

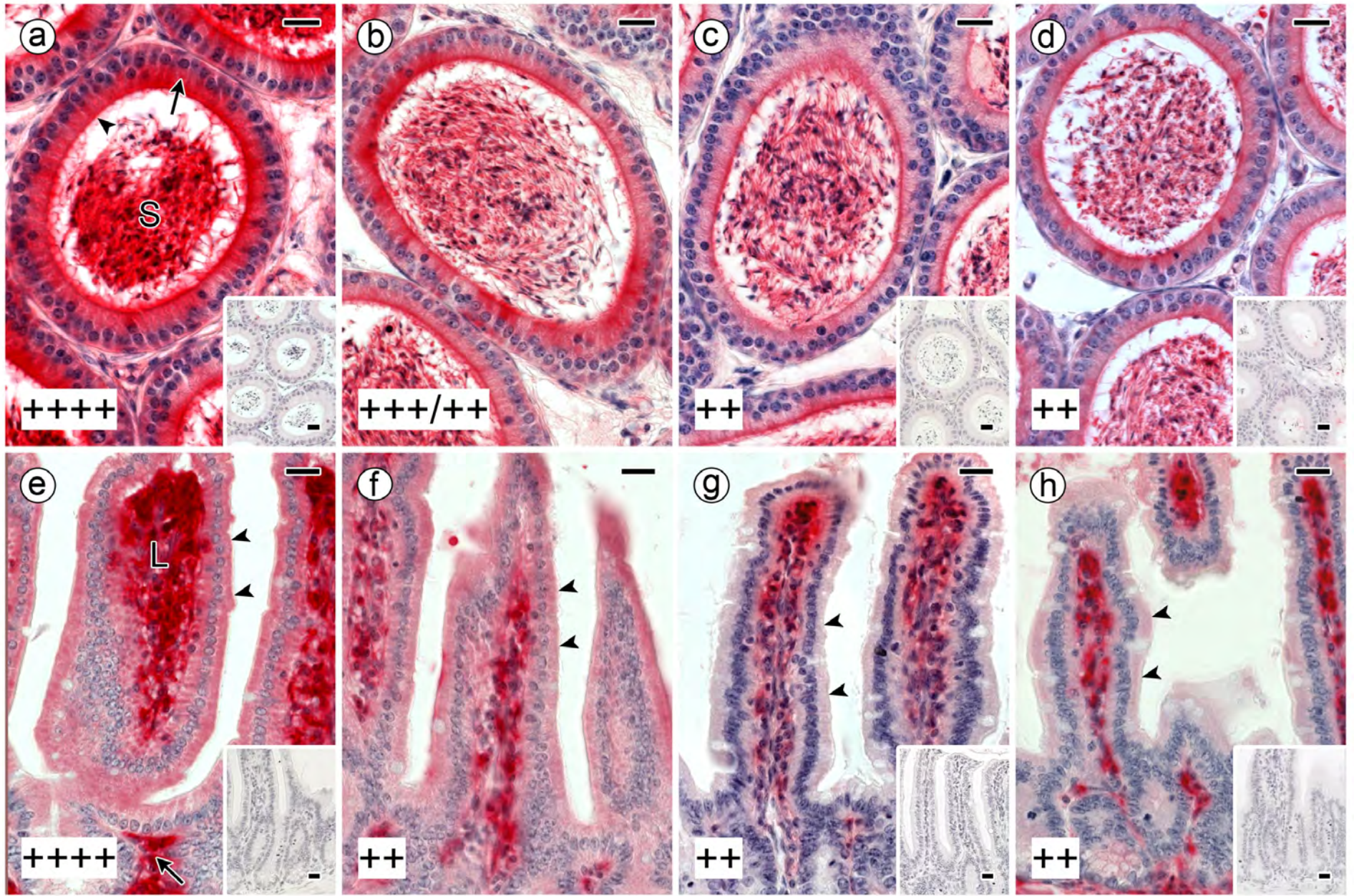


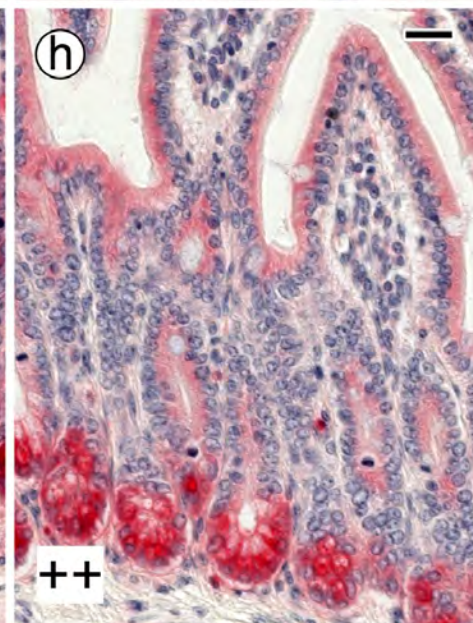
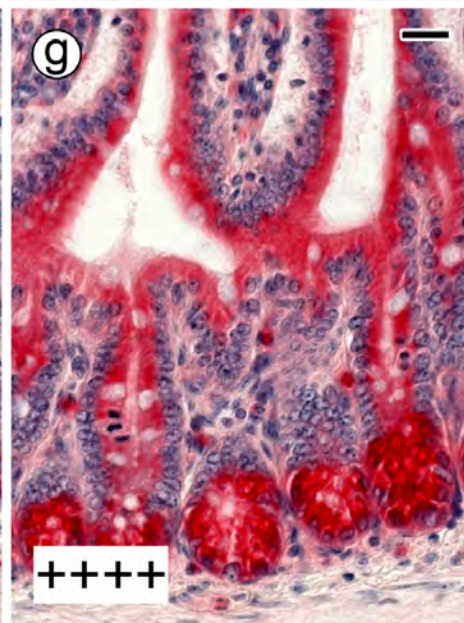
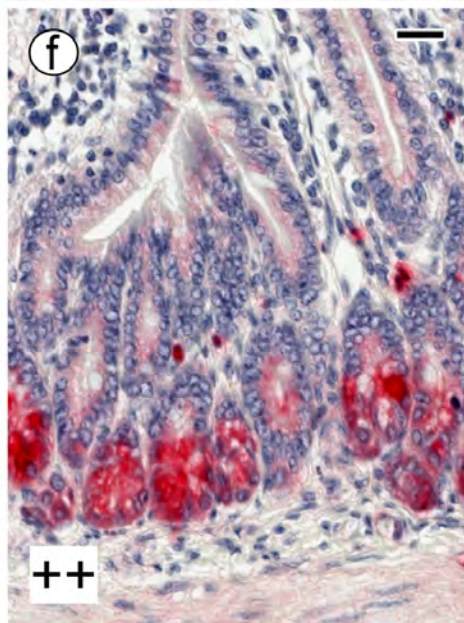
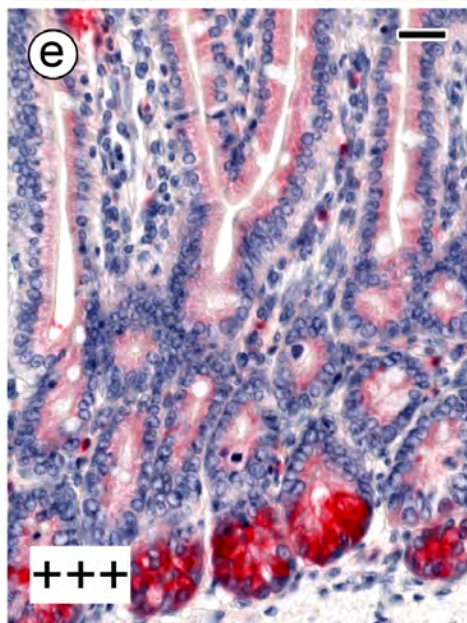
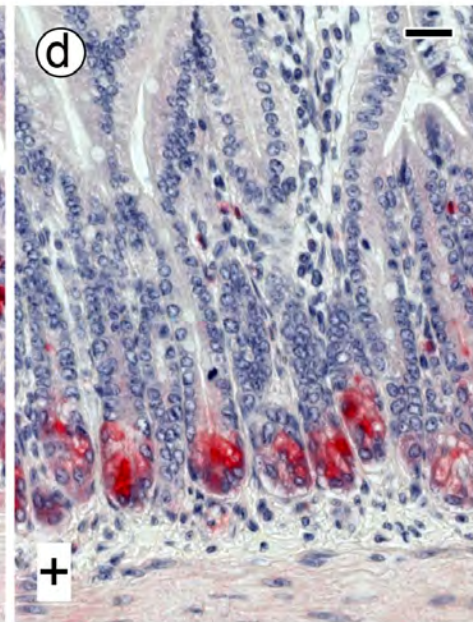
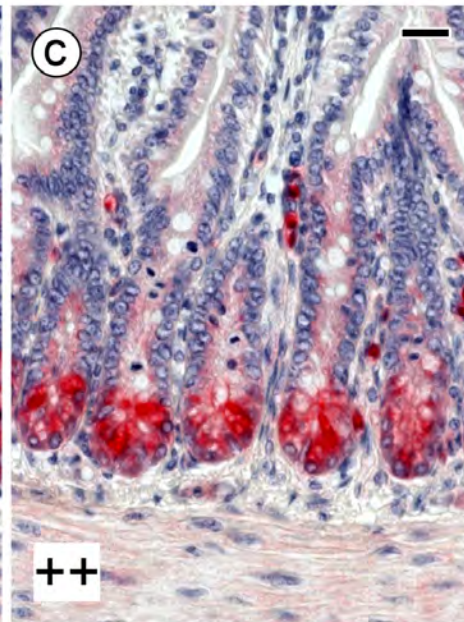
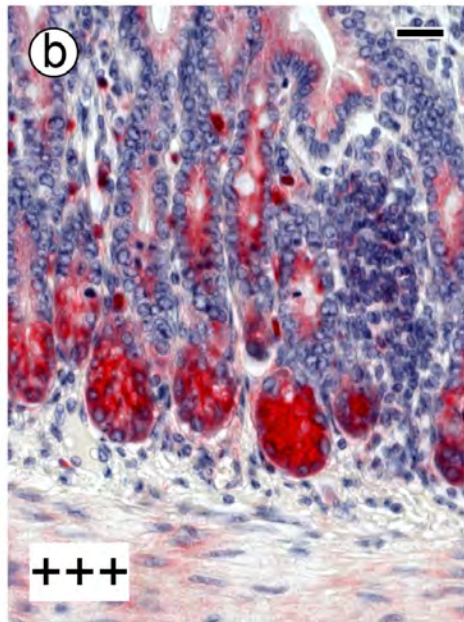
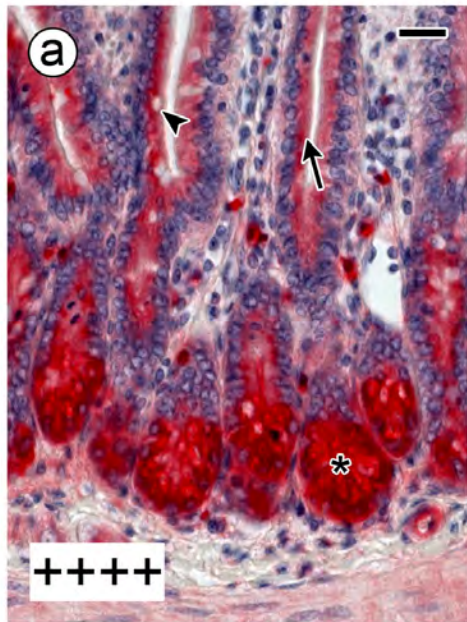
9, 11

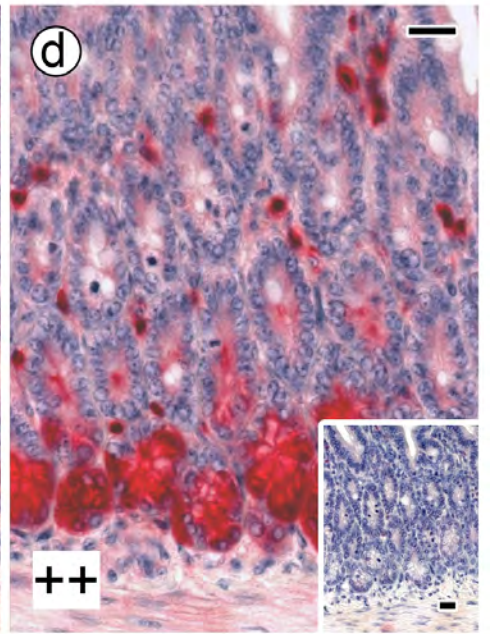
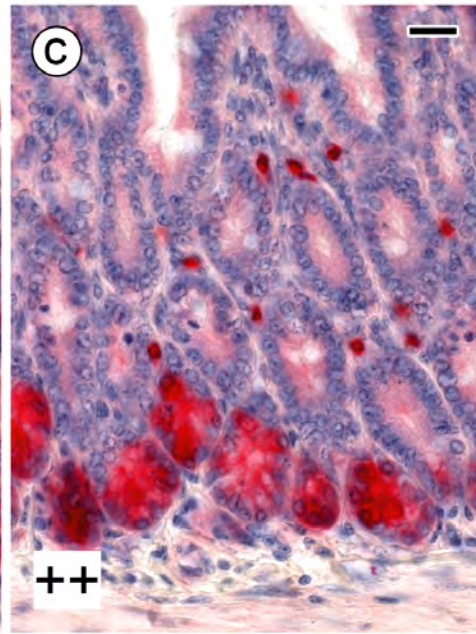
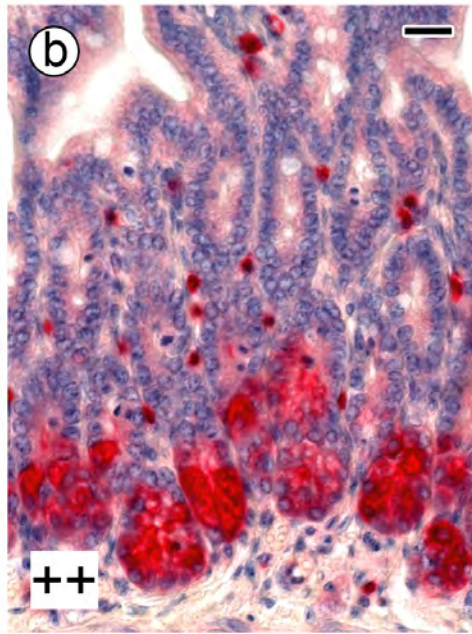
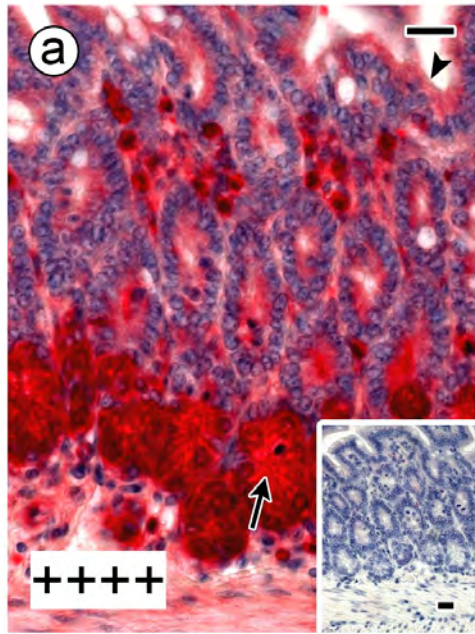












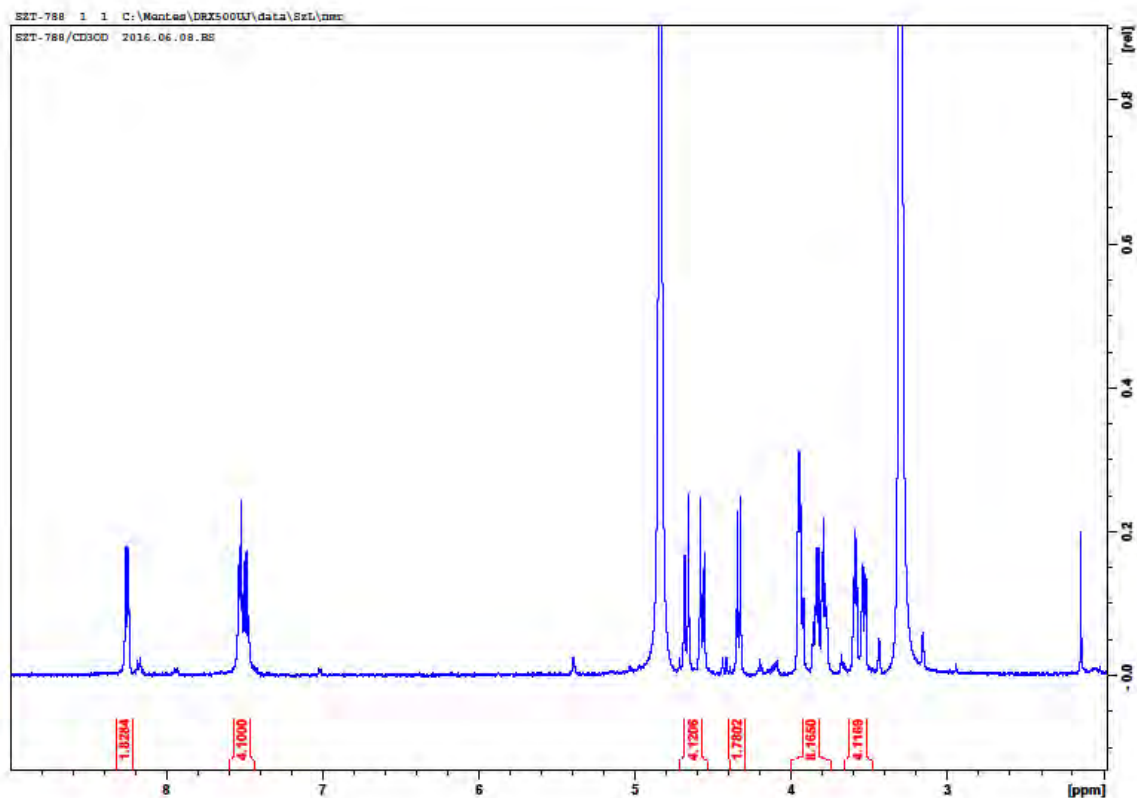


## Highlights

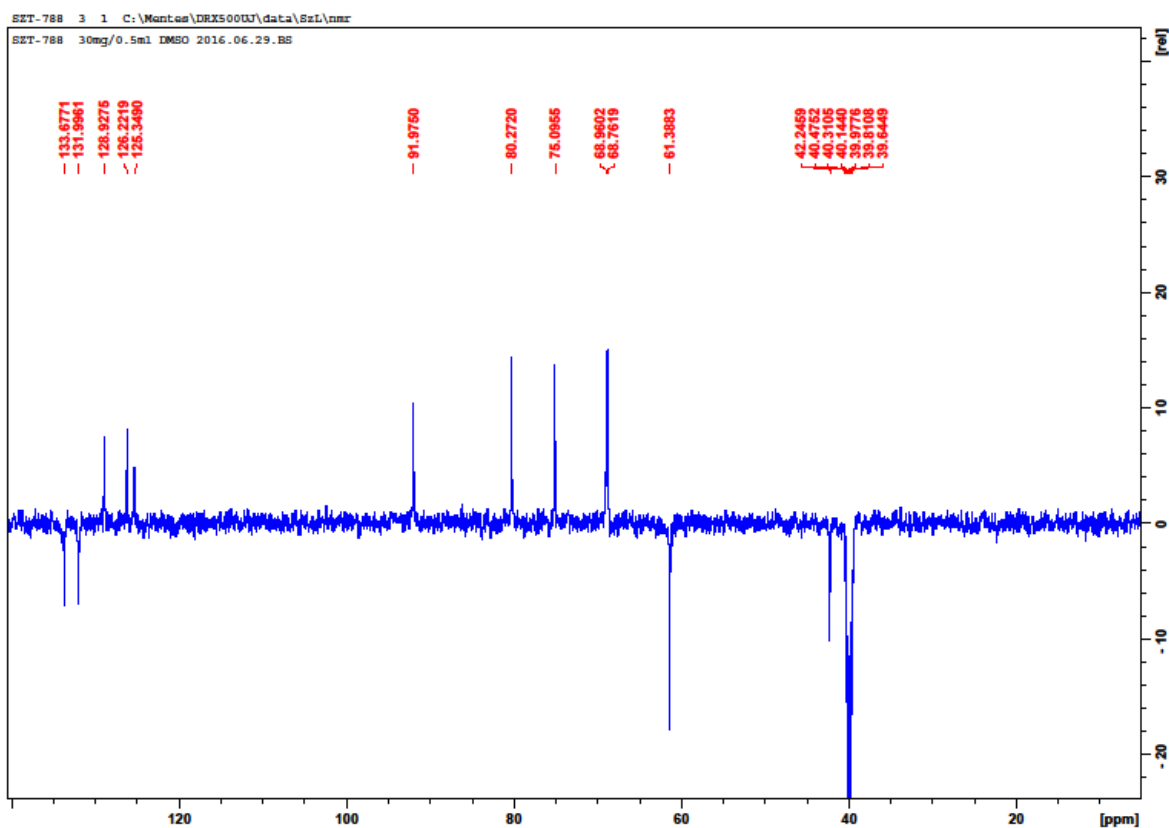
- Bivalent glycoside disulfides and selenides on an aromatic core are lectin inhibitors
- Headgroup presentation for cross-linking lectins has high flexibility and dynamics
- Inhibiting lectin staining in tissue sections is a close-to-in vivo assay

## Supporting Info to

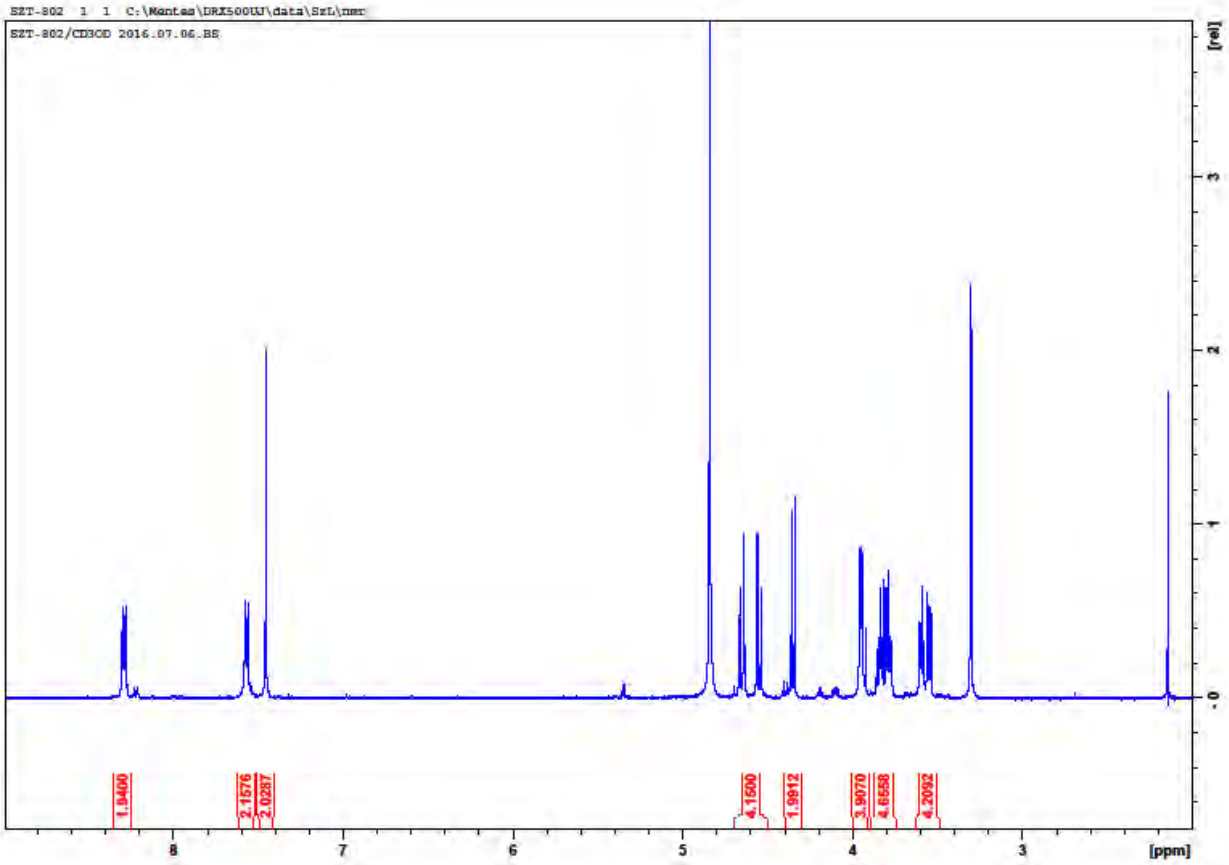
Bivalent *O*-glycoside mimetics with *S/disulfide/Se* substitutions and aromatic core: synthesis, molecular modeling and inhibitory activity on biomedically relevant lectins in assays of increasing physiological relevance  
by Herbert Kaltner,<sup>a,\*</sup> Tamás Szabó,<sup>b,\*</sup> Krisztina Fehér,<sup>c,\*</sup> Sabine André,<sup>a</sup> Sára Balla,<sup>b</sup> Joachim C. Manning,<sup>a</sup> László Szilágyi<sup>b,#</sup> and Hans-Joachim Gabius<sup>a,#</sup>



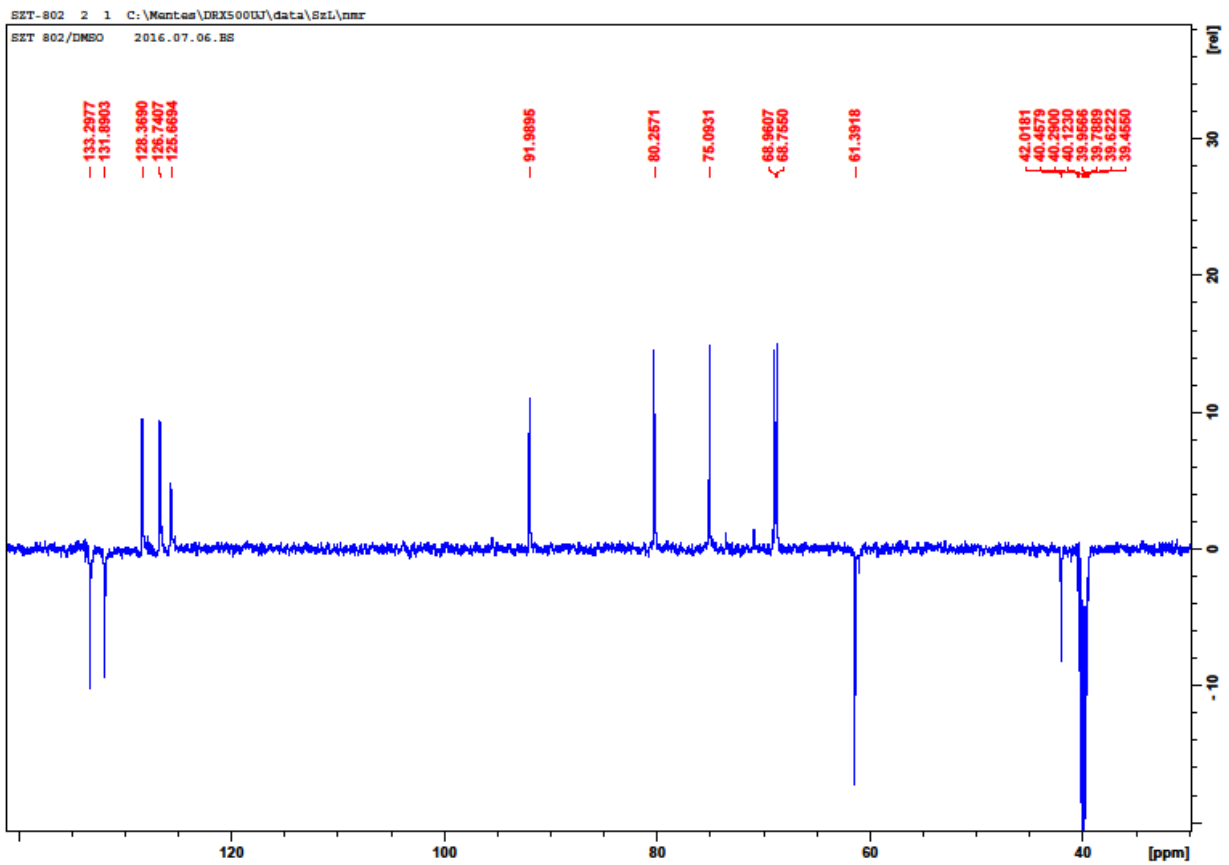
<sup>1</sup>H NMR spectrum of **1** in methanol-*d*<sub>4</sub>



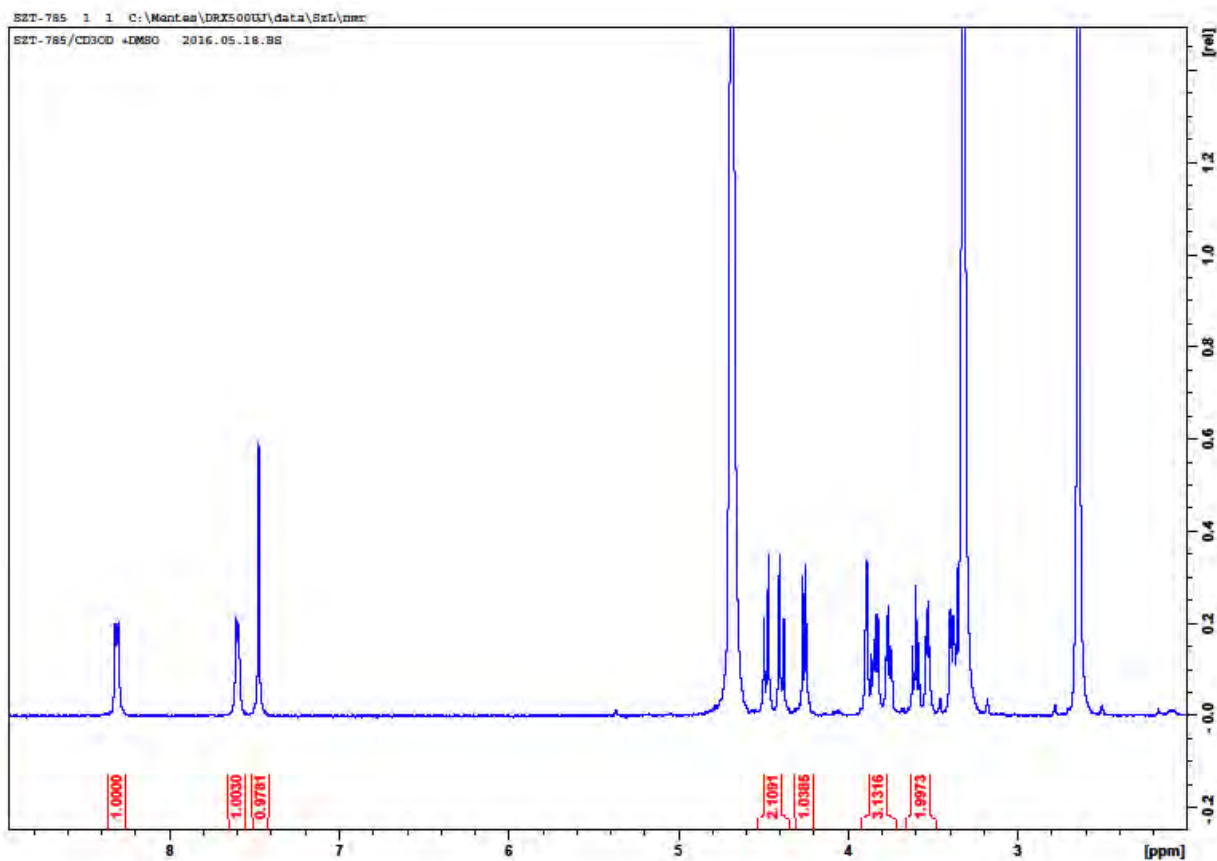
<sup>13</sup>C NMR spectrum of **1** in DMSO-*d*<sub>6</sub>



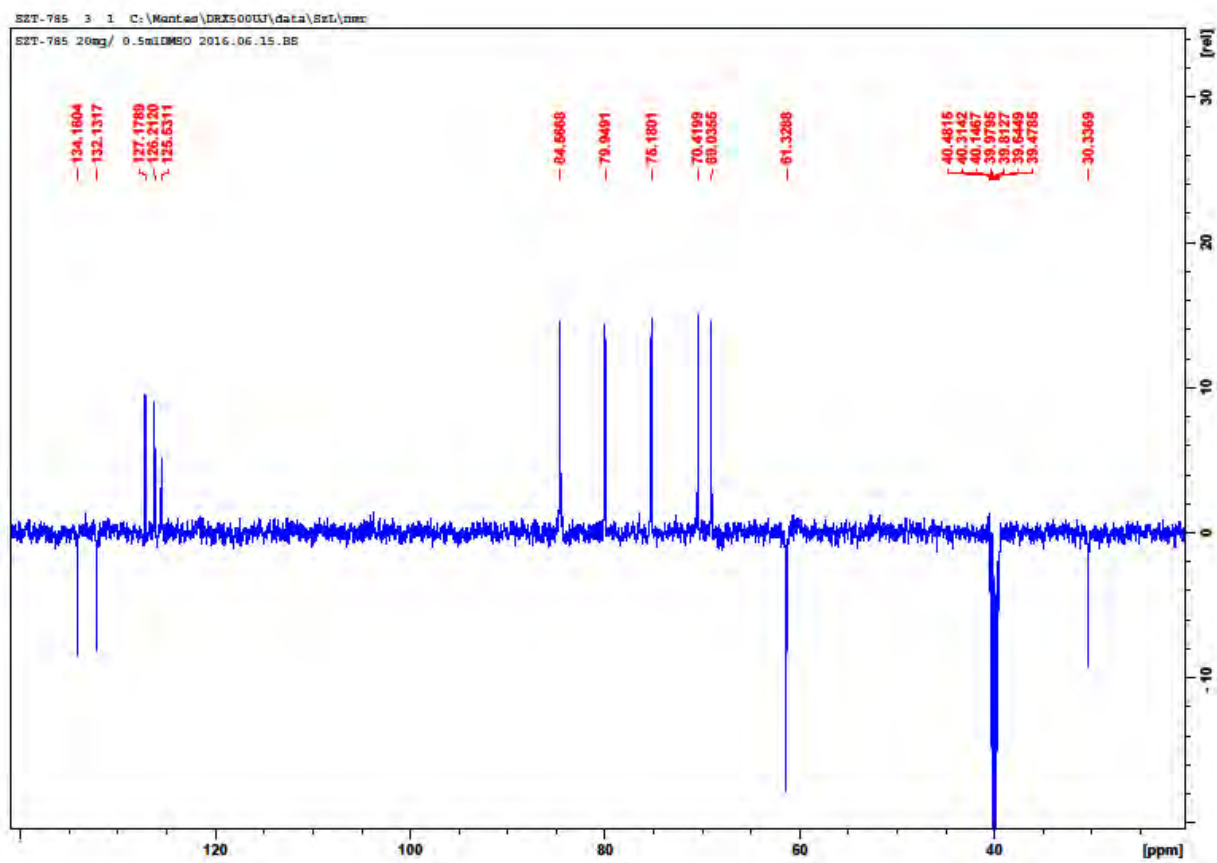
$^1\text{H}$  NMR spectrum of **2** in methanol- $d_4$



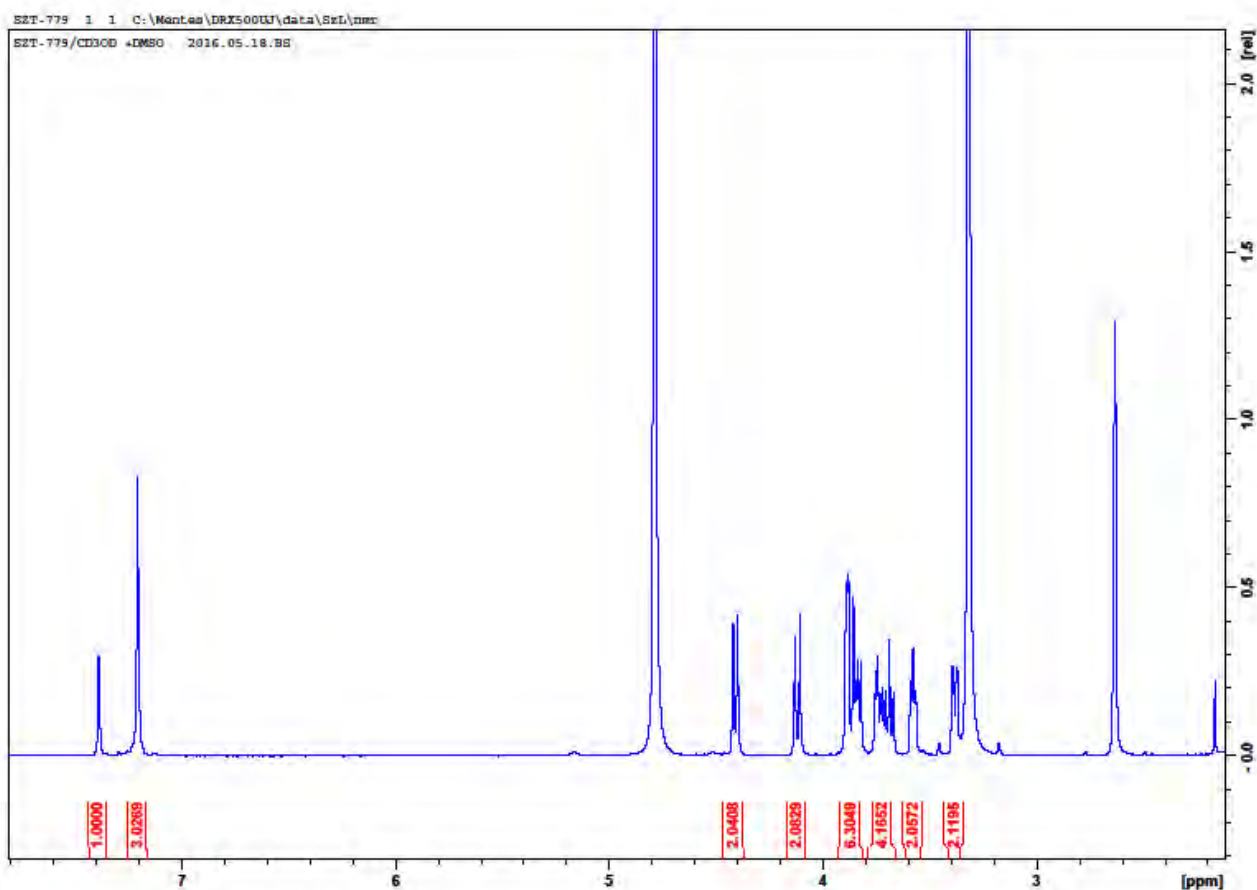
$^{13}\text{C}$  NMR spectrum of **2** in DMSO- $d_6$



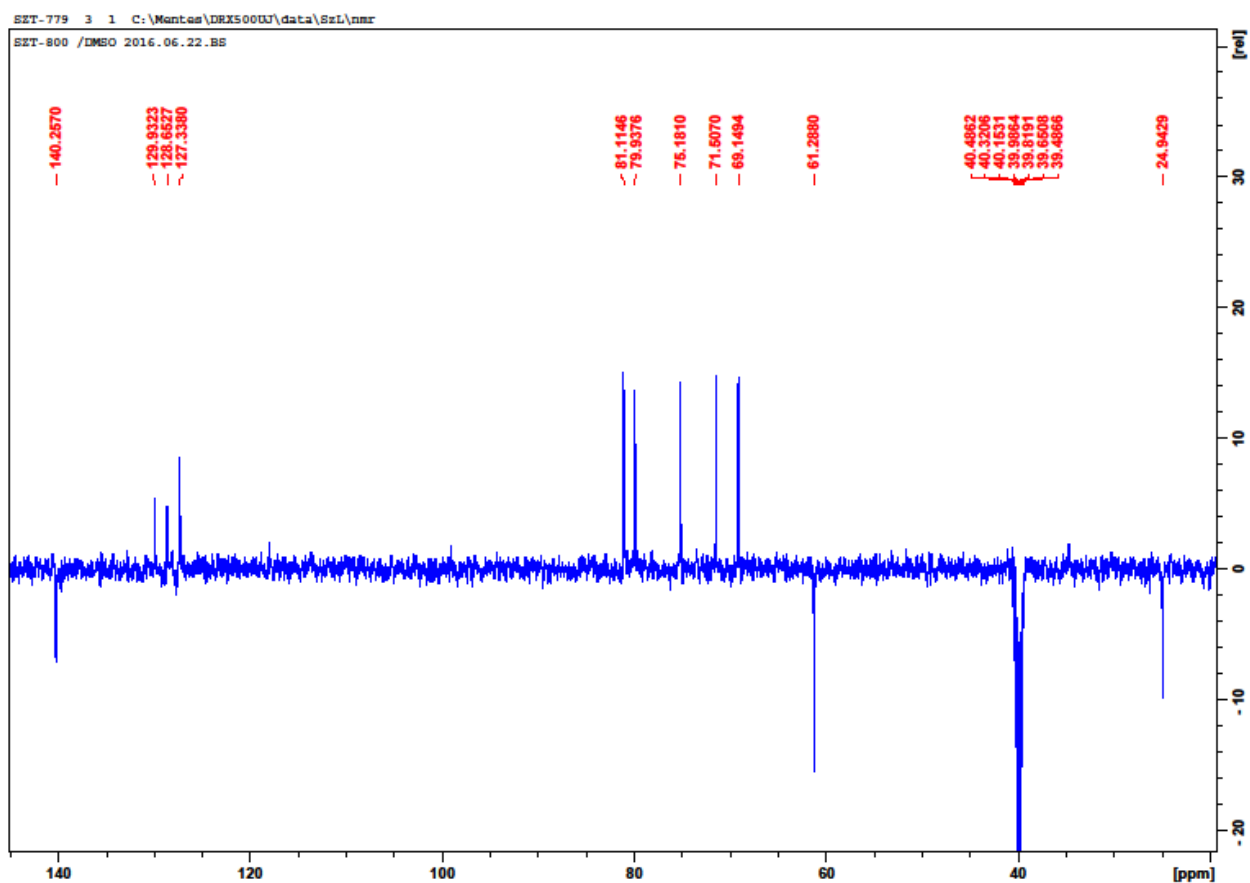
$^1\text{H}$  NMR spectrum of **3** in methanol- $d_4$



$^{13}\text{C}$  NMR spectrum of **3** in DMSO- $d_6$



$^1\text{H}$  NMR spectrum of **4** in methanol- $d_4$



$^{13}\text{C}$  NMR spectrum of **4** in DMSO- $d_6$